loaded by chemical conjugation. The tricomponent complexes thus generated were shown to induce robust antiparasitic immunity [4].

In this proof-of-concept study to evaluate the vaccine efficacy of the tricomponent complex against viral infections, we exploited a mouse infection model of Japanese encephalitis (JE). We have previously reported that the recombinantly produced envelope (E) protein of the JE virus (JEV) confers substantial protection against lethal JEV infection in mice [7]. In this study, we expressed the C-terminal one-third of the E protein (domain III [D3]) in *E. coli* and loaded it onto the COMP–Z fusion protein by chemical conjugation. We also created a tricomponent fusion complex in which the D3 antigen, COMP coiled-coil domain, and Z domain were genetically connected in sequence. We then evaluated the vaccine efficacy of the tricomponent complex generated either by chemical or genetic fusion, using a mouse model of lethal JEV infection.

2. Materials and methods

2.1. Production of COMP–Z/D3 tricomponent complex by chemical conjugation

The expression and purification of the JEV E protein D3 and COMP–Z fusion proteins from *E. coli* were as described previously [4,7]. Briefly, purified D3 was pyridyldithiol activated with *N*-succinimidyl 3-(2-pyridyldithio) propionate (SPDP; 0.6 mM; Thermo Scientific, Inc., Rockford, IL, USA). Concomitantly, the COMP–Z fusion protein was treated with dithiothreitol (DTT; 50 mM) to reduce the disulfide bonds located in the COMP coiled-coil domain. The modified D3 and COMP–Z were mixed in a 10:1 molar ratio at a total protein concentration of 1 mg/ml. The generated fusion complex was evaluated with a human IgG enzyme-linked immunosorbent assay (human IgG ELISA).

2.2. Production of D3–COMP–Z and Z–COMP–D3 tricomponent complexes by genetic fusion

First, the COMP-spacer coding region located between the *Nco*I and *Xho*I sites of the pET-22b vector (Merck KGaA, Darmstadt, Germany), described previously [4], was excised with the *Nco*I and *Xho*I restriction endonucleases and subcloned between the corresponding sites of the pET-21d vector (Merck KGaA). This subcloning removed the pelB signal from the COMP-spacer coding region. Next, to construct the pET-21d–Spacer1–COMP–Spacer2 expression plasmid (Figs. 2a and 3a), two overlapping oligonucleotides encoding the Spacer1 region (#1 sense and #2 antisense oligonucleotides) were annealed and subcloned at the unique *Nco*I site on the formerly constructed pET-21d–COMP–spacer expression plasmid. The two overlapping oligonucleotides were designed to generate an *Nco*I staggered end at the N-terminus but not at the C-terminus of the Spacer1 coding region, to reconstitute a unique *Nco*I site in the vector to allow further subcloning of the JEV D3 or Z domain, as described below.

Second, the JEV D3 coding region was PCR amplified from a plasmid containing the JEV (strain Beijing-1; GenBank accession no. L48961) E protein coding region [7] using a set of primers (#3 sense and #4 antisense oligonucleotide set containing an *Nco*I site or #5 sense and #6 antisense oligonucleotide set containing an *Xho*I site). The PCR-amplified fragment was subcloned into the pCR2.1 vector (Invitrogen, Carlsbad, CA, USA), and then digested with *Nco*I or *Xho*I. The excised fragment was subcloned at the *Nco*I or *Xho*I site on the formerly constructed pET-21d–Spacer1–COMP–Spacer2 expression plasmid (Figs. 2a and 3a) to create the D3–COMP–Spacer2 or Spacer1–COMP–D3 coding region, respectively.

Third, a synthetic gene encoding the Z domain (Val1 to Lys58; Protein Data Bank accession no. 2SPZ) was PCR amplified from a plasmid containing the corresponding gene [4] using a set of primers (#7 sense and #8 antisense oligonucleotide set containing an *Xho*I site or #9 sense and #10 antisense oligonucleotide set containing an *Nco*I site). The amplified fragment was subcloned into pCR2.1, and then digested with *Xho*I or *Nco*I. The excised fragment was subcloned at the *Xho*I site on the formerly constructed pET-21d–D3–COMP–Spacer2 expression plasmid or the *Nco*I site on the pET-21d–Spacer1–COMP–D3 expression plasmid to create the D3–COMP–Z or Z–COMP–D3 coding region, respectively. Table 1 lists the oligonucleotides used in this study. The correctness of the nucleotide sequences of the constructed fusion genes was confirmed by DNA sequencing.

E. coli BL21(DE3) harboring the pET-21d–D3–COMP–Z or pET-21d–Z–COMP–D3 expression plasmid was cultured in LB broth containing ampicillin (100 μg/mL), and the protein expression was induced with 1 mM isopropylthio-β-galactoside (IPTG) for 16 h. After induction, the cells were collected by centrifugation (9600 × *g*, 30 min), and resuspended in phosphate-buffered saline (PBS). The cells were disrupted by sonication (20 min × 3; Output 4, Duty 70, Tomy UD-201, Tomy Seiko Co. Ltd., Tokyo, Japan), and centrifuged (10,000 × *g*, 30 min) to collect the inclusion bodies. The inclusion bodies were dissolved in 8 M urea and centrifuged (10,000 × *g*, 30 min) to remove the insoluble debris. The protein solution dissolved in 8 M urea was dialyzed stepwise against decreasing concentrations of urea (8–1 M) and finally against PBS. The dialyzed samples were evaluated with a human IgG ELISA and size-exclusion chromatography (0.8 ml/min flow rate, HiLoad 16/60 Superdex 75 pg column; GE Healthcare, Little Chalfont, UK), as previously described [4]. Final recombinant protein yield was determined by bicinchoninic acid (BCA) assay. Protein samples which were PBS-exchanged, and then size-fractionated by size-exclusion chromatography (i.e., pentameric as well as high-molecular mass protein fractions), or unfractionated protein samples were used for human IgG ELISA experiments or mouse immunization studies.

2.3. Human IgG ELISA

Human IgG ELISA was conducted as previously described with a slight modification [4]. Briefly, 5 μg/ml human IgG (Sigma–Aldrich, St. Louis, MO, USA), diluted with bicarbonate buffer (15 mM Na_2CO_3, 35 mM $NaHCO_3$, pH 9.6; 50 μl/well), was applied to a 96-well microtiter plate (Sumilon; Sumitomo Bakelite Co., Ltd., Tokyo, Japan) and incubated at 4 °C overnight. The plate was blocked with 10% skim milk in PBS for 1 h at 37 °C. Chemically or genetically produced tricomponent protein samples (2 μg total protein/well) were added to the wells and incubated at 37 °C for 1 h, and then incubated with 50 μg/ml human IgG at 37 °C for 1 h to mask any unbound free Z domain. Mouse anti-His tag antibody (1:4000; GE Healthcare) or mouse anti-D3 antiserum (1:4000) was applied and incubated for 1 h at 37 °C. Then, anti-mouse IgG conjugated to alkaline phosphatase (1:4000; Sigma–Aldrich), followed by *p*-nitrophenylphosphate (Bio-Rad Laboratories Inc., Redmond, WA, USA) was added and incubated at 37 °C for 20 min. The optical density at 415 nm (OD_{415}) was measured with a microplate reader (Bio-Rad).

2.4. Immunization of mice

Seven-week-old female BALB/c mice (Japan SLC, Shizuoka, Japan), with 12–21 mice per group, were subcutaneously (s.c.) injected three times with D3 alone, a mixture of D3 and COMP–Z, the COMP–Z/D3 tricomponent complex (chemical conjugation), D3–COMP–Z or Z–COMP–D3 (genetic fusion) at weeks 0, 2,

Table 1
Oligonucleotides used in this study.

Oligonucleotide number	Nucleotide sequence
#1	5′-CATGGGTCCGGGCCCGGGTGGCGGTGGCAGCCACCATCACCATCACCACGGTGGCGGTGGCAGCGGTCCGGGCCCGGG-3′
#2	5′-CATGCCCGGGCCCGGACCGCTGCCACCGCCACCGTGGTGATGGTGATGGTGGCTGCCACCGCCACCCGGGCCCGGACC-3′
#3	5′-CGCCCATGGACAAACTGGCTCTGAAAGGCACA-3′
#4	5′-GCGCCATGGCCGTGCTTCCAGCCTTGTACCA-3′
#5	5′-CGCCTCGAGGACAAACTGGCTCTGAAAGGCACA-3′
#6	5′-GCGCTCGAGTTACGTGCTTCCAGCCTTGTACCA-3′
#7	5′-GCGCTCGAGGTGGATAACAAATTTAATAAAGAACAGC-3′
#8	5′-GCGCTCGAGTTATTTCGGGGCCTGTGCATCG-3′
#9	5′-GCGCCATGGTGGATAACAAATTTAATAAAGAACAG-3′
#10	5′-GCGCCATGGCTTTCGGGGCCTGTGCATCG-3′

The underlined sequences indicate restriction enzyme recognition sites.

and 4. Aluminum hydroxide (Imject Alum Adjuvant, Thermo Scientific, Inc.) was used as the adjuvant. For tricomponent complexes generated by genetic fusion, either unfractionated protein, high-molecular-mass fraction, or pentamer fraction was used as immunization material. All immunization samples contained equivalent amounts of D3 (30 μg). The amount of D3 protein moiety contained in the tricomponent complexes was calculated based on the molecular mass ratio between the D3 protein moiety and the whole fusion protein. The amount of total protein contents in the immunization samples was measured by BCA assay. As a positive control, a mouse-brain-derived formalin-inactivated JE vaccine (strain Beijing-1; Chemo-Sero-Therapeutic Research Institute, Kumamoto, Japan) was administered twice intraperitoneally (i.p.) to 7-week-old female BALB/c mice in a volume of 100 μl with 3-day interval at week 4, according to the manufacturer's protocol. Blood samples were collected at week 6 from the tail vein for the virus neutralization test.

Animal experimental protocols were approved by the Institutional Animal Care and Use Committee (the internal ethics registration number: 4995) and animal experiments were conducted according to the institutional ethical guidelines for animal experiments.

2.5. Virus neutralization test

A virus-neutralizing antibody assay was conducted as described previously with a 50% focus reduction neutralization test ($FRNT_{50}$) [7]. Briefly, 10 μl of virus solution was mixed with 10 μl of serially diluted heat-inactivated antiserum. The mixture was incubated at 28 °C for 2 h and then added to BHK-21 cell monolayers. The plates were incubated further at 37 °C for 2 h under 5% CO_2. After incubation, 80 μl of medium containing 0.8% methylcellulose (Wako Pure Chemical Industries, Osaka, Japan) was added and incubated in a CO_2 incubator at 37 °C for 24 h. The cells were fixed with methanol, and incubated with rabbit anti-JE antiserum and goat anti-rabbit horseradish-peroxidase-conjugated IgG (Cappel Laboratories, Inc., Cochranville, PA, USA). The color reaction was developed with 0.01% H_2O_2 and 3–3′-diaminobenzidine tetrahydrochloride (Wako) in PBS.

2.6. Viral challenge

The JEV infection experiments were conducted as described previously [7]. Briefly, 2 weeks after the last immunization (at week 6), the mice were challenged i.p. with 1×10^5 focus-forming units (FFU) of JEV strain JaGAr01 (50 LD_{50}) immediately after an intracerebral (i.c.) injection of 50 μl of PBS. The mice were monitored daily until day 28 after infection for behavioral and physical symptoms, such as paralysis, and their survival data were recorded.

2.7. Statistical analysis

Statistically significant differences were determined with the Wilcoxon–Mann–Whitney test for the virus-neutralizing antibody titers. The Kaplan–Meier log-rank test was used to compare the survival curves of the control group and a specified immunization group, or two specific immunization groups. Statistical analyses were conducted with JMP software version 8.0 (SAS Institute Inc., Cary, NC, USA).

3. Results and discussion

Many safe and potent vaccines include live attenuated and killed pathogens, but it may be preferable in some cases to mount immune responses against specific antigens or epitopes derived from the target pathogens, rather than to mount broad responses to large repertoires of structural units of the pathogenic organisms. In these cases, subunit vaccines consisting of specific antigens, designed and produced by recombinant DNA technology, provide formidable advantages. However, highly purified innocuous protein antigens require adjuvants to induce sufficient levels of immunity for protection against lethal pathogenic infections.

The adjuvants most widely used with robust safety are aluminum salts. Nevertheless, recent human clinical trials (for example, in malaria vaccine development [8]) have indicated that alum adjuvants are often insufficiently strong to induce an antibody response to recombinant-protein-based subunit vaccines. Therefore, the development of stronger and safe adjuvants is urgently required. It is also true that stronger adjuvants are more likely to induce stronger reactogenicity, so the development of novel adjuvants represents a formidable challenge. Soluble innocuous proteins alone are very weakly immunogenic, first because they do not contain pathogen-associated molecular patterns (PAMPs) that can elicit an innate immune response, which are prerequisites for the efficient induction of adaptive immunity [9]. Second, antigens that do not represent particulate structures are weak inducers of B-cell activation [10]. Third, antigens that are not efficiently taken up by professional APCs are likely to be cleared from the system without eliciting strong adaptive immunity [2]. Therefore, increasing the protein mass by forming multimers [11] or particulate structures is a promising and practically feasible way to transform innocuous recombinant proteins into potent subunit vaccines [12]. For this reason, we have recently developed a novel vaccine platform technology, designated the "tricomponent immunopotentiating system" (TIPS) [4], to meet all the important criteria required for the creation of effective recombinant vaccines. To evaluate the immunogenic efficacy of TIPS, we first demonstrated that the COMP–Z fusion complex loaded with the *Plasmodium vivax* ookinete surface protein, Pvs25, a transmission-blocking candidate vaccine for *P. vivax* malaria, or the C-terminal 19-kDa fragment of *P. yoelii* merozoite surface protein-1 (MSP1-19), an antigen expressed

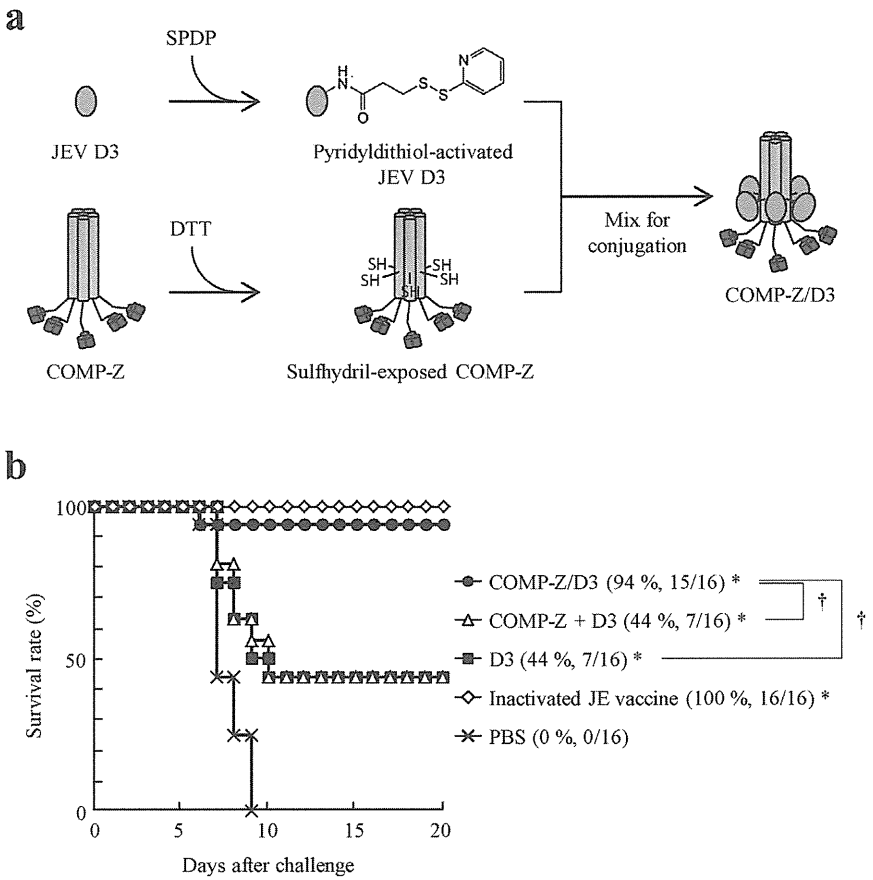

Fig. 1. Generation of the chemically conjugated COMP–Z/D3 tricomponent complex and its protective efficacy against a lethal Japanese encephalitis virus (JEV) infection in mice. (a) *Escherichia coli*-expressed recombinant D3 protein was treated with the heterobifunctional cross-linking reagent *N*-succinimidyl 3-(2-pyridyldithio) propionate (SPDP) to modify its primary amines. Simultaneously, the *E. coli*-expressed COMP–Z delivery molecule [4] was treated with dithiothreitol (DTT) to generate free sulfhydryl groups at the cysteine residues located near the C-terminal region of the COMP coiled-coil motif. These two proteins were mixed for conjugation to generate the COMP–Z/D3 tricomponent complex. (b) The protective efficacy of the COMP–Z/D3 tricomponent complex against a lethal JEV infection was evaluated. Seven-week-old female BALB/c mice (16 mice per group) were subcutaneously injected three times with D3 alone, a mixture of D3 and COMP–Z, or the COMP–Z/D3 tricomponent complex at weeks 0, 2, and 4. Aluminum hydroxide was used as the adjuvant. Two weeks after the third immunization, the mice were challenged with 1×10^5 FFU of JEV strain JaGAr01 (50 LD_{50}) via an intraperitoneal (i.p.) route. To increase the cerebral infectivity of the virus, 50 μl of PBS was injected intracerebrally immediately before the i.p. viral challenge. The mice were monitored for 3 weeks after infection for signs of behavioral or physical abnormalities and their survival rates were recorded. Survival rates are expressed in percentages; the numbers of surviving mice per total number of challenged mice are given in parentheses. D3, unloaded D3 protein; COMP–Z + D3, a mixture of COMP–Z and D3. $^*P < 0.01$ vs. PBS group; $^\dagger P < 0.01$ between the two indicated groups analyzed with the log-rank test.

in the asexual stage of a rodent malarial parasite, induced robust antiparasite immunity [4].

In the present study, we selected a mouse JEV infection model for a proof-of-concept evaluation of the TIPS platform technology to determine whether it can be applied to the development of vaccines for viral infections. We previously demonstrated that the JEV E protein expressed in *E. coli* confers potent protection against lethal JEV infection in mice [7]. In the present study, we selected the JEV E protein D3, which constitutes the C-terminal one-third of the E protein, because this domain was more stable as a water-soluble form and is more efficiently produced when expressed in *E. coli* than the full-length E protein. Therefore, it confers a formidable advantage when it is manipulated to create the chemical or genetic fusion complex.

To load D3 onto COMP–Z, the protein was first treated with the heterobifunctional cross-linker SPDP to generate pyridildithiol-activated D3, and was then mixed with DTT-treated COMP–Z for conjugation (Fig. 1a). Because the COMP coiled-coil domain contains cysteine residues, the reduced sulfhydryls reacted with the pyridildithiol-activated D3 to generate the tricomponent complex COMP–Z/D3. The generated complex retained its immunoglobulin-binding domain (IBD) function, confirmed by human IgG ELISA (data not shown). Next, BALB/c mice were immunized s.c. with the COMP–Z/D3 complex, and the animals were subjected to lethal infection with JEV. In our mouse JEV infection protocol, the i.p. administration of 1×10^5 FFU (50 LD_{50}), followed by an i.c. injection of PBS, consistently killed 100% of naïve mice or PBS (mock)-administered mice within 1–2 weeks after infection, whereas i.p. immunization with a formalin-inactivated JE vaccine provided complete protection [7]. We demonstrated that immunization with the COMP–Z/D3 complex conferred 94% protection (15/16) (Fig. 1b). On the contrary, immunization with D3 alone or D3 not integrated into the tricomponent complex (i.e., a mixture of D3 and COMP–Z) conferred only 44% protection (7/16) (Fig. 1b). This seminal study indicated that loading a viral antigen onto the COMP–Z delivery vehicle robustly augmented immunogenicity of the antigen, a result consistent with our previous observation of malaria parasite antigens [4].

Genetic fusion is generally considered superior to chemical conjugation for the generation of homogeneous molecules. However, malaria parasite antigens, such as Pvs25, composed of a series of epidermal-growth-factor-like domains, are difficult to produce in *E. coli* as recombinant antigens that retain their native folds. Therefore, we previously had no choice but to use chemical conjugation to load the parasite antigens onto COMP–Z [4]. In contrast, given that both D3 and COMP–Z could be expressed in *E. coli* at

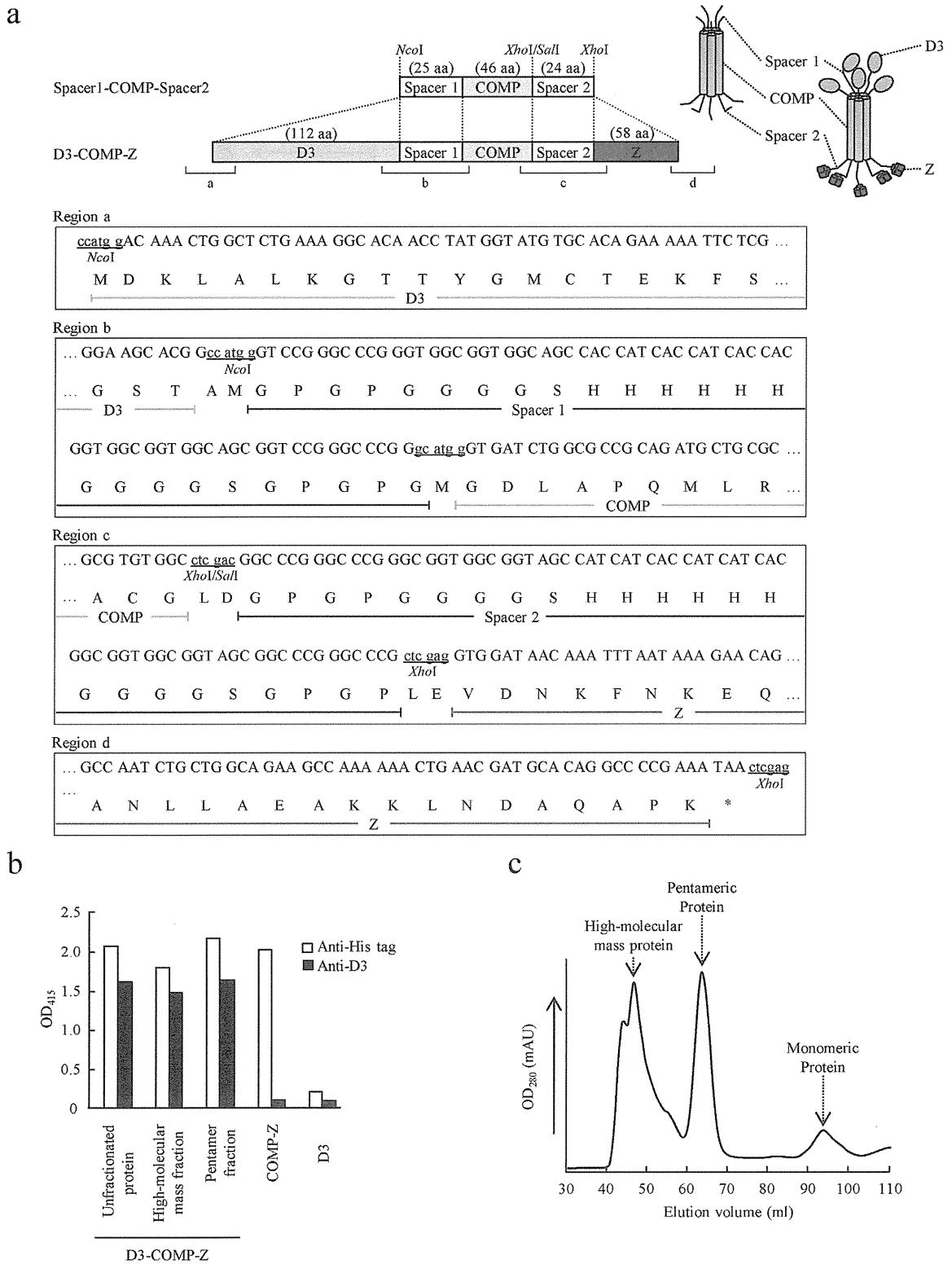

Fig. 2. Generation of the genetically conjugated D3–COMP–Z tricomponent complex. (a) A schematic drawing of the D3–COMP–Z tricomponent genetic fusion complex: Spacer1–COMP–Spacer2, the COMP coiled-coil domain (46 amino acids of $COMP_{27–72}$) containing the N- and C-terminal spacer sequences (designated "Spacer 1" and "Spacer 2", respectively); D3–COMP–Z, Spacer1–COMP–Spacer2 fused to the D3 coding sequence at the N-terminus and the Z-domain coding sequence at the C-terminus. Regions a–d indicate the nucleotide and amino acid sequences of the corresponding regions of the fusion complex. The Spacer1–COMP–Spacer2 sequence was inserted between the *Nco*I and *Xho*I sites of the pET-21d vector. The D3 protein and Z-domain coding regions were inserted at the *Nco*I and *Xho*I sites, respectively, of the pET-21d–Spacer1–COMP–Spacer2 expression plasmid. (b) Unfractionated and fractionated proteins were analyzed with a human IgG ELISA using anti-His tag (open bars) or anti-D3 (filled bars) antiserum to confirm the integrity of the tricomponent complex. (c) The D3–COMP–Z fusion protein was fractionated by size-exclusion chromatography to separate the pentamers from the high-molecular-mass protein species for the immunization study.

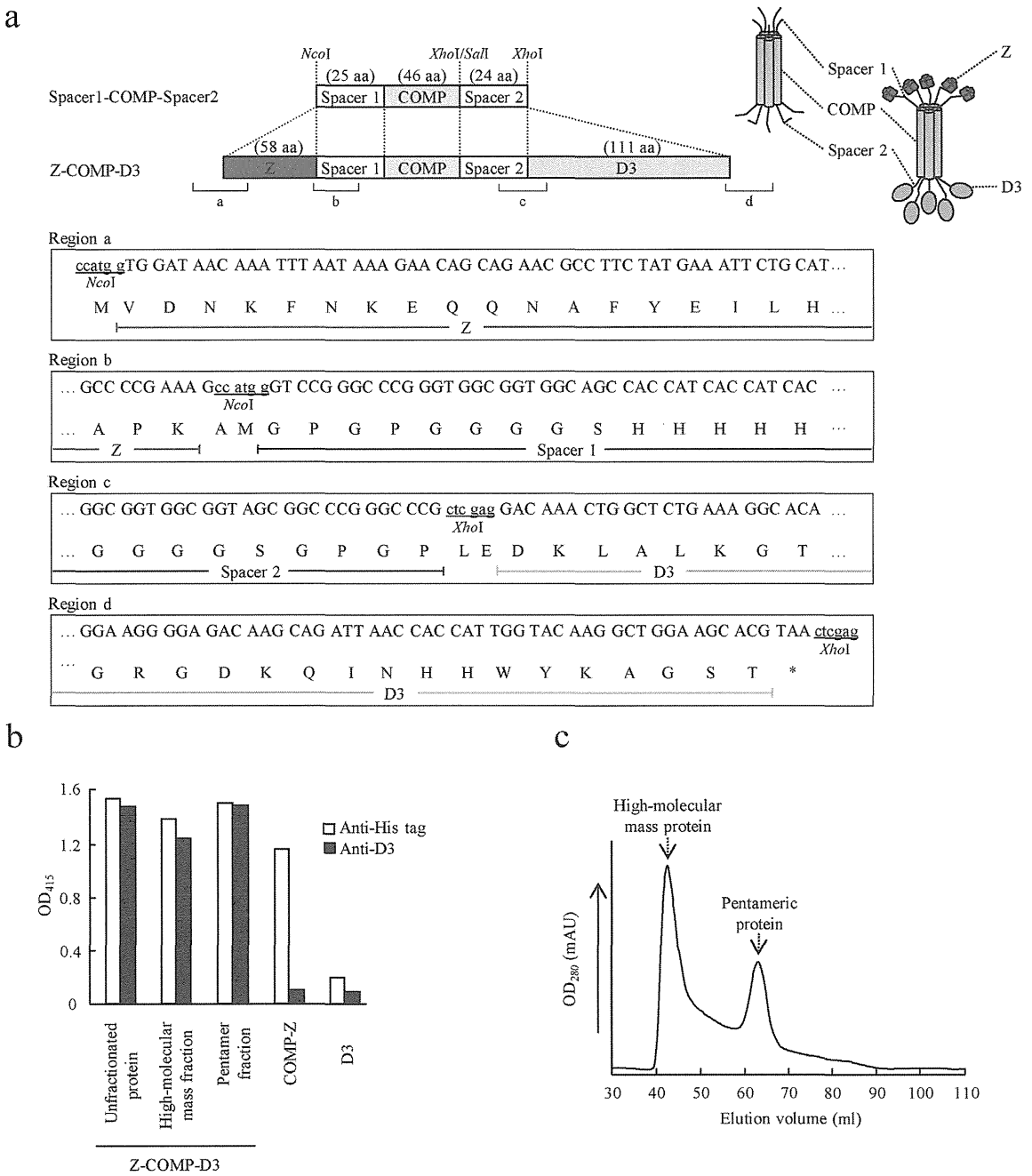

Fig. 3. Generation of the genetically conjugated Z–COMP–D3 tricomponent complex. (a) A schematic drawing of the Z–COMP–D3 tricomponent genetic fusion complex: Spacer1–COMP–Spacer2, see legend of Fig. 2a; Z–COMP–D3, the Spacer1–COMP–Spacer2 fused to the Z-domain coding sequence at the N-terminus and the D3 coding sequence at the C-terminus. Regions a–d indicate the nucleotide and amino acid sequences of the corresponding regions of the fusion complex. The Z domain and D3 protein coding regions were inserted at the *Nco*I and *Xho*I sites, respectively, of the pET-21d–Spacer1–COMP–Spacer2 expression plasmid. (b) Unfractionated and fractionated proteins were analyzed with a human IgG ELISA using anti-His tag (open bars) or anti-D3 (filled bars) antiserum to confirm the integrity of the tricomponent complex. (c) The Z–COMP–D3 fusion protein was fractionated by size-exclusion chromatography to separate the pentamers from the high-molecular-mass protein species for the immunization study.

substantial levels, retaining their biological functions, we investigated whether genetic conjugation was feasible for generating the tricomponent complex. To this end, we constructed two types of tricomponent complex, in which the positions of D3 and Z were switched: D3–COMP–Z and Z–COMP–D3 (Figs. 2a and 3a). These fusion proteins were produced in *E. coli* as inclusion bodies, but upon solubilization with 8 M urea followed by dialysis against PBS, they refolded to regain their D3 antigenicity and IBD functions (Figs. 2b and 3b; Supplemental Figs. 1a and b), which indicated that the Z domain was also refolded to its native configuration by the refolding process. Size-exclusion chromatography revealed that both pentameric and high-molecular-mass protein species were produced (Figs. 2c and 3c). We observed only homogeneous pentamers of the antigen-unloaded COMP–Z [4] and a tricomponent complex in which a short protein epitope of only 25 amino acids derived from human T-cell leukemia virus 1 was genetically fused to COMP–Z, but no high-molecular-mass protein species were detected (unpublished data). These results suggest that the D3 protein moiety of the tricomponent complex, which might not have completely refolded to its native conformation, has a tendency to aggregate, and functions as an aggregation core to generate high-molecular-mass molecules. An additional advantage of genetically

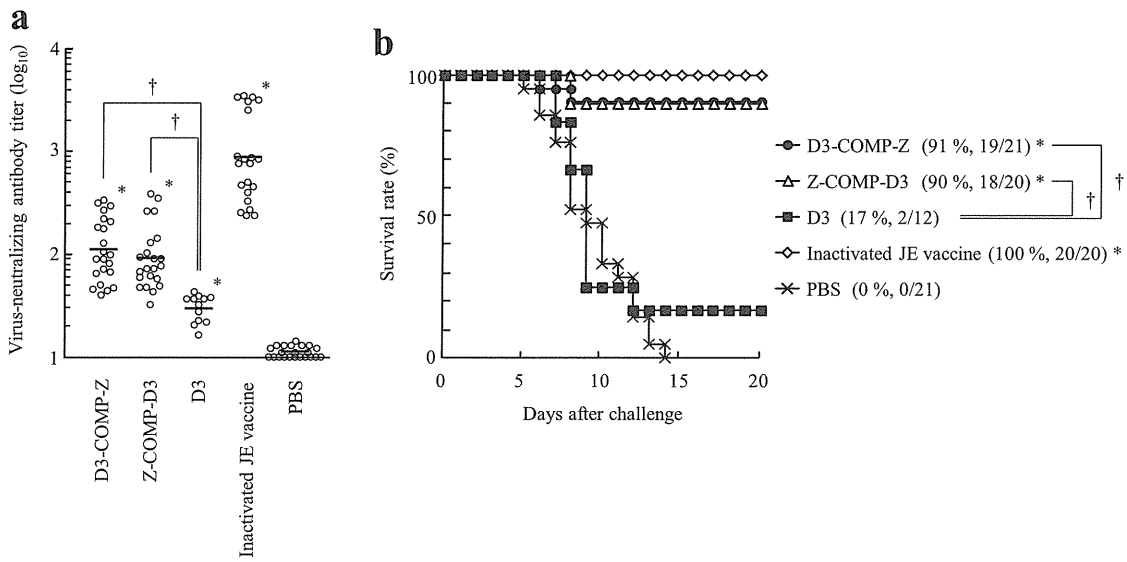

Fig. 4. Vaccine efficacies of the pentameric D3–COMP–Z and Z–COMP–D3 tricomponent complexes. (a) JEV-neutralizing antibody titers for the antisera collected at week 6. Female BALB/c mice were immunized with the pentameric D3–COMP–Z or Z–COMP–D3 fusion complex (fractions 60–70 mL collected by size-exclusion chromatography presented in Fig. 2c or 3c, respectively), each dose of which was calculated to include 30 μg of the D3 protein moiety. The immunization schedule and infection protocol were identical to those described in the legend of Fig. 1b. $^{*}P < 0.01$ vs. PBS group; $^{\dagger}P < 0.01$ between the two indicated groups analyzed with the Wilcoxon–Mann–Whitney test. (b) Protective efficacy of the tricomponent complexes against a lethal JEV infection, as described in the legend of Fig. 1b. Survival rates are expressed in percentages; the numbers of surviving mice per total number of infected mice are also provided in parentheses. $^{*}P < 0.01$ vs. PBS group; $^{\dagger}P < 0.01$ between the two indicated groups analyzed with the log-rank test.

fusing D3 to COMP–Z is that its water solubility is significantly improved compared with that of the D3 protein alone. The D3 protein showed a tendency to form insoluble aggregates upon repeated freeze-and-thaw processes, whereas both D3–COMP–Z and Z–COMP–D3 did not. This is a considerable advantage in vaccine manufacture, and this biochemical characteristic is probably attributable to the high water solubility of the COMP–Z molecule.

Supplementary material related to this article can be found, in the online version, at http://dx.doi.org/10.1016/j.vaccine.2013.12.016.

The final protein yield for the PBS-exchanged D3–COMP–Z and Z–COMP–D3 was 50 mg/L and 100 mg/L of bacterial culture, respectively, for unfractionated whole protein, 30 mg/L and 16 mg/L for the high-molecular-mass protein species, respectively, and 12 mg/L and 48 mg/L for the pentamer species, respectively.

We have previously demonstrated that all three constituent components of TIPS are essential to induce effective immune responses [4]. To confirm that this is also true for the D3-based JE vaccine model, we attempted to create fusion proteins lacking the Z domain. However, after solubilization in 8 M urea, the D3–COMP and COMP–D3 fusion proteins were subjected to a refolding process by dialysis against PBS, and they immediately formed aggregations. This was not observed for the D3 protein alone, so we presumed that the multimerization of D3 by the pentameric COMP coiled-coil domain significantly facilitated the aggregation process. Therefore, we concluded that the Z domain is essential for antigen delivery [4], and that in some cases, the Z domain is essential to improve the water solubility of the complex to avoid the formation of insoluble aggregates.

Finally, we immunized mice with the pentameric tricomponent complexes, which had been separated from high-molecular-mass protein species by size-exclusion chromatography. Immunization materials used for this experiment were fractions 60–70 mL collected by size-exclusion chromatography (Figs. 2c and 3c), and the materials contained alum adjuvant. As shown in Fig. 4a, immunization with the pentameric D3–COMP–Z or Z–COMP–D3 tricomponent complex induced significantly elevated JEV-neutralizing antibodies compared with unloaded D3 protein. Furthermore, when the immunized mice were challenged with a lethal dose of JEV, approximately 90% of the animals survived (Fig. 4b). In contrast, unloaded D3 conferred only 17% protection (Fig. 4b), indicating that the integration of the antigen into the tricomponent complex robustly augmented its protective efficacy against viral infection. This result is consistent with the data presented in Fig. 1. We also tested the vaccine efficacy of unfractionated tricomponent complexes as well as high-molecular-mass protein species (fractions 40–50 mL in Figs. 2c and 3c) mixed with alum adjuvant. Immunization with unfractionated whole protein conferred comparable levels of protection, i.e., 91% for D3–COMP–Z and 84% for Z–COMP–D3 (Table 2). Immunization with the high-molecular mass protein species also showed almost comparable levels of protection (Table 2). Immunization with the tricomponent complexes not containing alum adjuvant generally conferred 20–40% lower protection levels (data not shown), confirming that protein multimerization, APC-targeting, and innate immunity induction properties of vaccine formulations are necessary to be combined for the better vaccine efficacy. The unfractionated proteins contained high-molecular-mass protein species, which were soluble aggregates of the complex. As mentioned above, the soluble aggregates might have been generated by incompletely folded D3 protein, which functioned as a

Table 2
JEV challenge experiments conducted by using unfractionated whole protein or high-molecular-mass fraction of the tricomponent complexes mixed with alum adjuvant.

Immunization material	Unfractionated whole protein	High-molecular mass fraction
D3–COMP–Z	20/22 (91%)	8/9 (88.8%)
Z–COMP–D3	16/19 (84%)	6/8 (75.0%)
Inactivated JE vaccine	20/20 (100%)	10/10 (100%)
PBS	0/21 (0%)	0/9 (0%)

Data are expressed as the number of survived mice per total number of mice infected with a lethal dose of JEV (50 LD_{50}).

hydrophobic aggregation core. It is assumed that incompletely folded proteins less efficiently provide the native protective epitopes recognized by B lymphocytes. However, high-molecular-mass proteins show a tendency to induce higher antibody responses than low-molecular-mass proteins containing the same epitopes [10]. Therefore, these conflicting effects might have offset one another to maintain the level of protective immunity against viral infection.

In this study, we created two types of a genetically fused complex, D3–COMP–Z and Z–COMP–D3, in which the only difference was the relative positions of D3 and Z. Both constructs showed similar D3 antigenicity and IBD functions (Figs. 2b and 3b), chromatographic profiles (Figs. 2c and 3c), immunogenicity (Fig. 4a), and vaccine efficacy (Fig. 4b). These results indicate that the Z domain can function as the IBD when placed at either the N- or C-terminus of the COMP coiled-coil moiety. This was also true for the D3 antigen. However, depending on the vaccine proteins to be fused, masking the N- or C-terminus may negatively affect the protein folding, consequently affecting the efficacy of the vaccine. If this is the case for a given protein of interest, then either the COMP–Z or Z–COMP can be chosen as the better fusion partner.

Protection against lethal JEV infection is primarily mediated by neutralizing antibodies. Therefore, molecular design optimized to induce virus particle-specific antibodies with virus-neutralizing capacity is paramount importance for creating effective JE vaccines. Fig. 4a shows that virus-neutralizing antibody titers attained by the complexes are significantly higher than 10. In the $FRNT_{50}$, antibody titers above 10–20 are considered seropositive and could potentially provide protection against the lethal virus infection. Immunization with the D3 protein with alum adjuvant conferred only 17% of protection, but the tricomponent complexes were 90% protective (Fig. 4b). This difference in protective efficacy could be explained by the difference in virus-neutralizing antibody titers, which were significantly different between these two vaccine materials (titers: 30 vs. 100). For the inactivated JE vaccine the virus-neutralizing antibody titer approached 1000, which was high enough to provide complete protection against the lethal virus infection (Fig. 4b). Although titers for the tricomponent complexes were much lower than the titer attained by the JE vaccine, we reasoned that titers around 100 provide high levels of protection against the lethal virus infection.

Although commercial JE vaccines exist, there have been several promising attempts to create next-generation JE vaccines. For example, Alka et al. [13] reported that D3 protein produced in *E. coli* as a His-tag or maltose-binding-protein fusion protein conferred approximately 80% protection against lethal JEV challenge infection when administered to mice with an aluminum hydroxide adjuvant. Wu et al. [14] reported that immunization with a D3–thioredoxin fusion protein with incomplete Freund's adjuvant or cationic liposomes conferred 60% or 80% protection in mice, respectively. Verma et al. [15] reported that immunization with D3 with Freund's adjuvant induced high levels of virus-neutralizing antibodies in mice. The inclusion of oil-based adjuvants is effective in immunization regimes for D3-based vaccines, although many of them are unsuitable for human use because of their potentially high reactogenicity. In contrast, aluminum-salt-based adjuvants have a long history of safe use in humans, but are often not strong enough to induce protective immunity when used with recombinant proteins. Therefore, a combination of protein delivery systems and aluminum salt adjuvants may provide a promising solution to the provision of strong protective immunity by recombinant-protein-based vaccines.

In this study, we exploited an antigen-delivery molecule including the COMP coiled-coil domain and a B-lymphocyte targeting ligand to enhance the immunogenicity of the recombinant JEV E protein antigen, which is otherwise very weakly immunogenic. Our results clearly demonstrate that the JEV D3 antigen loaded onto the delivery molecule robustly augmented the antiviral immunity in a mouse model of JEV infection. The tricomponent complex is an efficient inducer of humoral immunity against the protein antigens loaded, as demonstrated in the present study of JEV infection and previously in models of malaria infection [4]. Therefore, it is reasonable to expect that there are other infections that could be effectively controlled by this vaccine platform technology, particularly those that are primarily controlled by antibodies. Further studies are underway to evaluate the versatility of the tricomponent complex for the design of subunit vaccines for infectious diseases.

Acknowledgements

This work was supported by the Program for the Promotion of Basic Research Activities for Innovative Biosciences from the Bio-oriented Technology Research Advancement Institution in Japan, and a Cooperative Research Grant from the Institute of Tropical Medicine, Nagasaki University, Japan.

References

[1] Banchereau J, Steinman RM. Dendritic cells and the control of immunity. Nature 1998;392:245–52.
[2] Caminschi I, Shortman K. Boosting antibody responses by targeting antigens to dendritic cells. Trends in Immunology 2012;33:71–7.
[3] Tacken PJ, Torensma R, Figdor CG. Targeting antigens to dendritic cells in vivo. Immunobiology 2006;211:599–608.
[4] Miyata T, Harakuni T, Tsuboi T, Sattabongkot J, Ikehara A, Tachibana M, et al. Tricomponent immunopotentiating system as a novel molecular design strategy for malaria vaccine development. Infection and Immunity 2011;79:4260–75.
[5] Efimov VP, Lustig A, Engel J. The thrombospondin-like chains of cartilage oligomeric matrix protein are assembled by a five-stranded alpha-helical bundle between residues 20 and 83. FEBS Letters 1994;341:54–8.
[6] Tashiro M, Tejero R, Zimmerman DE, Celda B, Nilsson B, Montelione GT. High-resolution solution NMR structure of the Z domain of staphylococcal protein A. Journal of Molecular Biology 1997;272:573–90.
[7] Tafuku S, Miyata T, Tadano M, Mitsumata R, Kawakami H, Harakuni T, et al. Japanese encephalitis virus structural and nonstructural proteins expressed in *Escherichia coli* induce protective immunity in mice. Microbes and Infection/Institut Pasteur 2012;14:169–76.
[8] Malkin EM, Durbin AP, Diemert DJ, Sattabongkot J, Wu Y, Miura K, et al. Phase 1 vaccine trial of Pvs25H: a transmission blocking vaccine for *Plasmodium vivax* malaria. Vaccine 2005;23:3131–8.
[9] Akira S. Innate immunity and adjuvants. Philosophical Transactions of the Royal Society of London Series B, Biological Sciences 2011;366:2748–55.
[10] Link A, Zabel F, Schnetzler Y, Titz A, Brombacher F, Bachmann MF. Innate immunity mediates follicular transport of particulate but not soluble protein antigen. Journal of Immunology (Baltimore, MD: 1950) 2012;188:3724–33.
[11] Wibowo N, Chuan YP, Lua LHL, Middelberg APJ. Modular engineering of a microbially-produced viral capsomere vaccine for influenza. Chemical Engineering Science 2013;103:12–20.
[12] Arakawa T. Adjuvants: no longer a 'dirty little secret', but essential key players in vaccines of the future. Expert Review of Vaccines 2011;10:1–5.
[13] Alka, Bharati K, Malik YP, Vrati S. Immunogenicity and protective efficacy of the *E. coli*-expressed domain III of Japanese encephalitis virus envelope protein in mice. Medical Microbiology and Immunology 2007;196:227–31.
[14] Wu SC, Yu CH, Lin CW, Chu IM. The domain III fragment of Japanese encephalitis virus envelope protein: mouse immunogenicity and liposome adjuvanticity. Vaccine 2003;21:2516–22.
[15] Verma SK, Gupta N, Pattnaik P, Babu JP, Rao PV, Kumar S. Antibodies against refolded recombinant envelope protein (domain III) of Japanese encephalitis virus inhibit the JEV infection to porcine stable kidney cells. Protein and Peptide Letters 2009;16:1334–41.

Virology 452-453 (2014) 117–124

Contents lists available at ScienceDirect

Virology

journal homepage: www.elsevier.com/locate/yviro

Preferential recognition of monomeric CCR5 expressed in cultured cells by the HIV-1 envelope glycoprotein gp120 for the entry of R5 HIV-1

Yusuke Nakano [a], Kazuaki Monde [a], Hiromi Terasawa [a], Yuzhe Yuan [b], Keisuke Yusa [b], Shinji Harada [a], Yosuke Maeda [a,*]

[a] Department of Medical Virology, Faculty of Life Sciences, Kumamoto University, 1-1-1 Honjo, Kumamoto 860-8556, Japan
[b] Division of Biological Chemistry and Biologicals, National Institute of Health Sciences, Kami-youga 1-18-1, Setagaya, Tokyo 158-8501, Japan

ARTICLE INFO

Article history:
Received 9 October 2013
Returned to author for revisions
30 October 2013
Accepted 23 December 2013

Keywords:
HIV-1
CCR5
Monomer
Oligomerization
Bimolecular fluorescence complementation assay
CCR5 antagonist

ABSTRACT

Bimolecular fluorescence complementation (BiFC) and western blot analysis demonstrated that CCR5 exists as constitutive homo-oligomers, which was further enhanced by its antagonists such as maraviroc (MVC) and TAK-779. Staining by monoclonal antibodies recognizing different epitopes of CCR5 revealed that CCR5 oligomer was structurally different from the monomer. To determine which forms of CCR5 are well recognized by CCR5-using HIV-1 for the entry, BiFC-positive and -negative cell fractions in CD4-positive 293T cells were collected by fluorescent-activated cell sorter, and infected with luciferase-reporter HIV-1 pseudotyped with CCR5-using Envs including R5 and R5X4. R5 and dual-R5 HIV-1 substantially infected BiFC-negative fraction rather than BiFC-positive fraction, indicating the preferential recognition of monomeric CCR5 by R5 and dual-R5 Envs. Although CCR5 antagonists enhanced oligomerization of CCR5, MVC-resistant HIV-1 was found to still recognize both MVC-bound and -unbound forms of monomeric CCR5, suggesting the constrained use of monomeric CCR5 by R5 HIV-1.

Introduction

Interaction of the outer envelope (Env) glycoprotein gp120 of human immunodeficiency virus type-1 (HIV-1) with CD4 and one of the coreceptors (either CCR5 or CXCR4) is essential for the entry of HIV-1 (reviewed in (Wilen et al., 2012)). Viruses that exclusively use CCR5 (R5 HIV-1) are transmission variants, and predominant throughout the course of infection. On the other hand, viruses that use CXCR4 emerge at late stage of infection, and are thought to be associated with CD4 depletion and disease progression in half of HIV-1-infected individuals (Connor et al., 1997; Scarlatti et al., 1997). Most of CXCR4-using viruses still use CCR5 (R5X4 HIV-1) while several variants exclusively use CXCR4 (X4 HIV-1).

Previous studies have shown that natural ligands such as macrophage inflammatory protein (MIP)-1α (CCL3), MIP-1β (CCL4), and RANTES (regulated on activation, normal T-cell expressed and secreted; CCL5) were able to inhibit R5 HIV-1 replication by steric hindrance or internalization of CCR5 (Alkhatib et al., 1997; Cocchi et al., 1995; Oberlin et al., 1996; Scarlatti et al., 1997). The antagonists of CCR5, such as TAK-779 and maraviroc (MVC), also interact with hydrophobic pocket of CCR5 formed by the transmembrane helices, and induce conformational changes in CCR5, thereby blocking entry of R5 HIV-1 (Dragic et al., 2000; Kondru et al., 2008; Maeda et al., 2006; Nishikawa et al., 2005; Seibert et al., 2006; Tsamis et al., 2003). The dimerization of CCR5 induced by anti-CCR5 mAb CCR5-02 was also reported to prevent the entry of R5 HIV-1 (Vila-Coro et al., 2000), suggesting the possible impact of dimerization or oligomerization of CCR5 on HIV-1 susceptibility. Although CCR5 was reported to exist as homo-oligomers without natural ligands (Benkirane et al., 1997; El-Asmar et al., 2005; Hammad et al., 2010; Issafras et al., 2002; Mellado et al., 2001; Sohy et al., 2009), it still remains to be determined whether oligomeric forms of CCR5 are structurally different from the monomeric forms, and affect entry efficiency of R5 HIV-1. It is also unknown whether CCR5 antagonists affect the oligomerization status of CCR5, whereas the CCR5 natural ligands have been shown to induce the dimerization of CCR5 (Chelli and Alizon, 2002; Hernanz-Falcon et al., 2004; Rodriguez-Frade et al., 1999; Vila-Coro et al., 2000). To address these issues, bimolecular fluorescence complementation (BiFC) assay was applied to detect homo-oligomeric forms of CCR5. Principally, BiFC assay is a non-invasive fluorescent-based technique that allows detection of protein-protein interactions in living cells (reviewed in (Kerppola, 2008)). BiFC assay is based on the association between two non-fluorescent fragments of a fluorescent protein when they are brought in proximity to each other by interaction between

* Corresponding author. Tel.: +81 96 373 5131; fax: +81 96 373 5132.
E-mail address: ymaeda@kumamoto-u.ac.jp (Y. Maeda).

0042-6822/$ - see front matter © 2013 Elsevier Inc. All rights reserved.
http://dx.doi.org/10.1016/j.virol.2013.12.034

proteins fused to the fragments. In our present study, by using BiFC, homo-oligomeric forms of CCR5 were detected to some extent without natural ligands, and further enhanced by CCR5 antagonists. In addition, susceptibility of sorted CCR5 oligomers-enriched cell fraction was found to be less susceptible compared to monomer-enriched fraction, indicating the preferential recognition of CCR5 monomer by R5 HIV-1.

Results

Detection of oligomeric forms of CCR5 without ligands

It has been shown that CCR5 exists as homo-oligomer without natural ligands such as CCL3, CCL4, and CCL5 (Benkirane et al., 1997; El-Asmar et al., 2005; Hammad et al., 2010; Issafras et al., 2002; Mellado et al., 2001; Sohy et al., 2009). However, it still remains to be determined whether oligomeric forms of CCR5 are structurally different from CCR5 monomer. To this end, BiFC assay was employed to detect oligomeric forms of CCR5. The CCR5 expression vectors fused to the N- and C-terminal fragments of green fluorescence protein (Kusabira–Green: KG) were constructed, and co-expressed in 293T cells. When the both proteins are expressed and close together, refolded KG protein results in KG signal. This fluorescent signal can be easily detected by flow cytometry or fluorescence microscopy. To analyze the structural differences between monomeric and oligomeric forms of CCR5, the cells were further stained with anti-CCR5 monoclonal antibodies (mAbs) recognizing different epitopes of CCR5 such as N-terminal (clones CTC8, 3A9), second extracellular domain (ECL2) (clones 2D7, 45531), or multiple conformation (clone 45549). As shown in the upper panel of Fig. 1, we were able to detect fluorescent (KG) signal using flow cytometry when both CCR5-KGN and CCR5-KGC were co-expressed in 293T cells, indicating the oligomerization of CCR5 without ligands. We also noticed that proportions of CCR5+KG+ subset were almost equal (24–26%) in all anti-CCR5 mAb clones (CTC8, 3A9, 2D7, and 45531) except the clone 45549. In contrast, CCR5+KG− subset was differentially stained by anti-CCR5 mAbs (Fig. 1, upper panel). The proportions of CCR5+KG− subset were high in the clones 2D7 and CTC8 (62% and 55%, respectively), intermediate in the clone 45531 (43%), and low in the clone 3A9 (26%). These results suggested that monomeric forms of CCR5 were structurally different from the oligomeric forms.

Enhancement of CCR5 oligomerization by CCR5 antagonists

Although natural ligands such as CCL3, CCL4, and CCL5 have been showing to induce oligomerization of CCR5 (Chelli and Alizon, 2002; Hernanz-Falcon et al., 2004; Rodriguez-Frade et al., 1999; Vila-Coro et al., 2000), it has not been determined how CCR5 antagonists such as TAK-779 or MVC affect the oligomerization of CCR5. Therefore, we also applied BiFC technique to check the effects of CCR5 antagonists on the oligomerization status of CCR5. After co-expressing CCR5-KGN and –KGC in 293T cells in the presence of MVC, the cells were stained with above-mentioned anti-CCR5 mAbs. The proportions of CCR5+KG+ subset were largely increased in all anti-CCR5 mAb clones (Fig. 1, lower panel) compared to those of the same fraction in the absence of ligands (Fig. 1, upper panel). Notably, the proportion of CCR5+KG+ subset was increased in the clone 45549 though its reactivity was quite low in the absence of ligands, confirming that conformational changes of CCR5 were indeed induced by MVC. To verify the enhancement of CCR5 oligomerization by CCR5 antagonists, we then checked whether another CCR5 antagonist TAK-779 enhanced oligomerization of CCR5. The CCR5-KG-expressing 293T cells were stained with 2D7 mAb that was able to equally detect both CCR5+KG− and CCR5+KG+ subsets as shown in Fig. 1, and KG-positive percentages in 2D7-positive population were determined by flow cytometry. We found that TAK-779 also enhanced the oligomerization of CCR5, while a CXCR4 antagonist AMD3100 had no effect (Fig. 2A). In particular, MVC had higher activity to enhance CCR5 oligomerization than TAK-779 in 293T cells. Western blot analysis using 293T cells expressing FLAG-tagged CCR5 with cross-linker indicated that CCR5 largely existed as monomer but also as dimer in the absence of ligands though lesser extent (Fig. 2B). It was also shown that MVC was able to induce expression of not only dimer but also more than dimer forms of CCR5. Notably, the level of CCR5 expression was up-regulated by MVC though the reason was uncertain. Native-PAGE analyses also revealed the similar results (Supplementary Fig. S1). The enhancement by CCR5 antagonists was also observed in different cell types such as HeLa, and NP2 cell lines though both had comparable activities in these cell lines (Supplementary Fig. S2). Dose-escalating study revealed that the concentrations

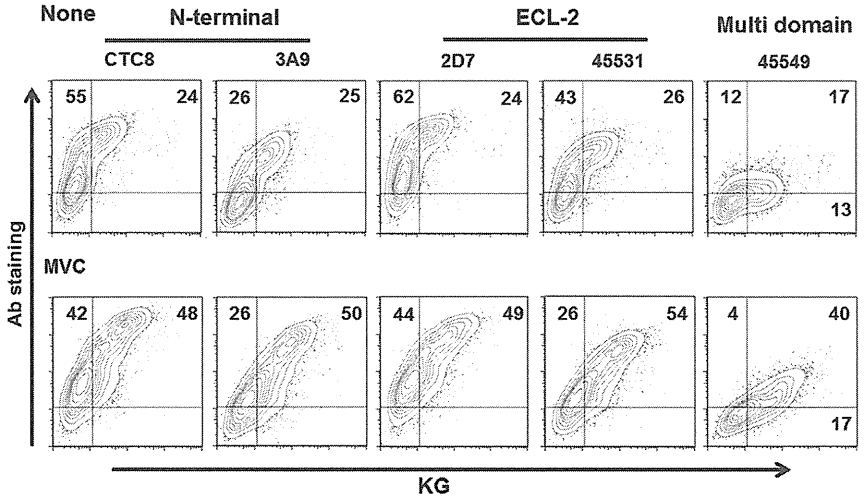

Fig. 1. Flow cytometry analyses of CCR5-KG-expressing 293T cells by anti-CCR5 mAbs in the presence or absence of MVC. The 293T cells were transfected with both CCR5-KG expression vectors, and incubated at 37 °C for 48 h in the absence of ligands (upper panel) or the presence of MVC at 2 μM (lower panel). Anti-CCR5 mAbs recognizing N-terminus (clones CTC8 and 3A9), ECL-2 (clone 2D7, 45531), and multiple domains (clone 45549) were used for the detection of CCR5, and analyzed by flow cytometry. The *y*-, and *x*-axes show the mean fluorescence intensity of CCR5 and KG, respectively. The number of each column shows the percent positive in each region.

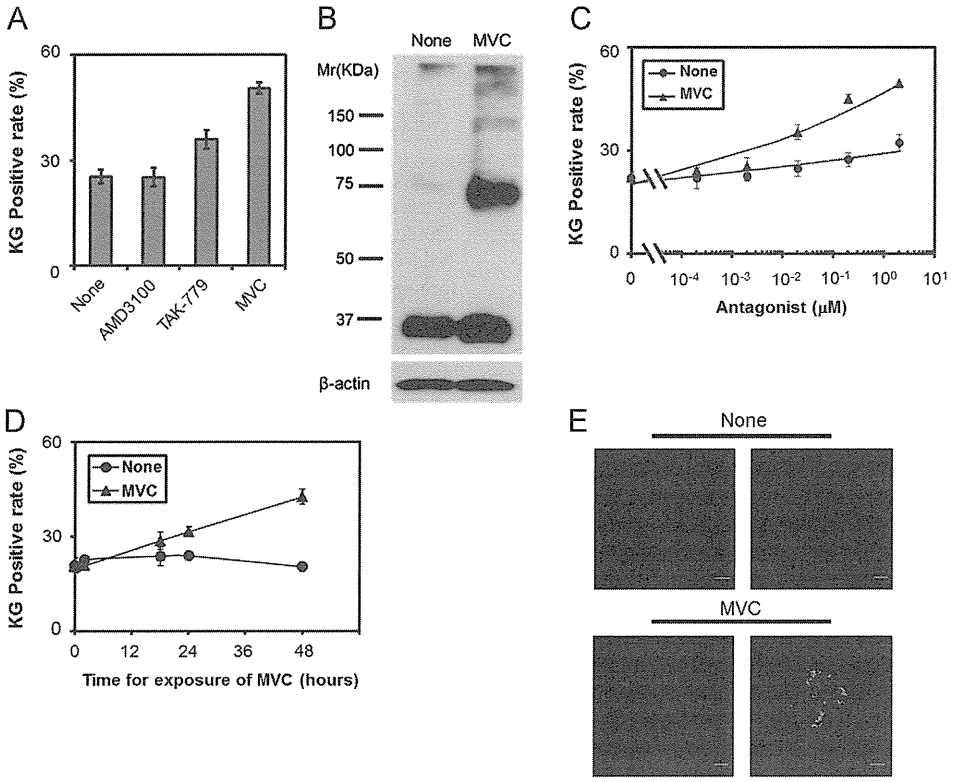

Fig. 2. Enhanced homo-oligomerization of CCR5 by CCR5 antagonists. (A) The 293T cells were transfected with expression vectors of CCR5-KG, and incubated in the presence or absence of AMD3100, TAK-779 or MVC at 2 μM each. The cells were stained with anti-CCR5 mAb 2D7, and analyzed by flow cytometry. The data shown represent the mean values of the percentage of KG-positive in 2D7-positive cell fraction ± standard deviations of three independent experiments. (B) The 293T cells were transfected with pCCR5-FLAG in the presence or absence of MVC. The cells were cross-linked by DSP, lysed, and analyzed by Western blot using anti-FLAG mAb. (C) Transfected cells were treated with increasing concentrations of TAK-779 or MVC ranging from 0.2 nM to 2 μM, and incubated at 37 °C for 48 h. The data shown represent the mean values of percent positive of KG ± standard deviations of three independent experiments. (D) The 293T cells expressing CCR5-KG were incubated at 37 °C for the indicated time of period in the presence of MVC (1 μM). Results are mean values of CCR5-KG positive rates ± standard deviations from experiments performed in triplicate. (E) Transfected HeLa cells with CCR5-KG were incubated in the absence (upper panel) or presence of MVC (lower panels) at 37 °C for 48 h, and fixed with 4% paraformaldehyde. Representative images in the middle sections of the cells are shown. Nuclear staining by DAPI is shown in blue. Scale bars correspond to 10 μm.

for enhanced oligomerization of CCR5 by TAK-779 or MVC were indeed corresponded to the inhibitory concentrations against HIV-1 infection (Fig. 2C). For example, in the case of MVC, the EC_{50} value of inhibitory activity against R5 HIV-1 (JR-FL) was 3.7 ± 1.4 nM (data not shown), while the EC_{50} value of activity to enhance oligomerization of CCR5 was 7.4 ± 5.1 nM, indicating that CCR5 could be oligomerized at enough concentrations for inhibiting R5 HIV-1 infection.

It has been shown that oligomerization of CCR5 was induced shortly after the addition of natural ligands as previously described (Chelli and Alizon, 2002; Hernanz-Falcon et al., 2004; Rodriguez-Frade et al., 1999; Vila-Coro et al., 2000). However, a time-course experiment showed that more than 24 h were necessary to enhance CCR5 oligomerization by MVC (Fig. 2D). Confocal laser scanning microscopy also showed that the CCR5-KG signals were located not only at the plasma membrane but also in the cytoplasm without ligands, and were further augmented by MVC (Fig. 2E). These results suggested that oligomerization of CCR5 needed de novo synthesis of CCR5 and occurred in the intracellular compartments before expressed on the cell surface.

Infection of KG-positive and -negative cell fractions with R5 HIV-1

Since the structures of oligomeric forms of CCR5 were possibly different from monomeric CCR5 as shown in Fig. 1, we next analyzed the abilities of R5 HIV-1 to recognize monomeric and oligomeric forms of CCR5. To this end, we first stained CD4-positive 293T cells expressing CCR5-KGN and –KGC with anti-CCR5 mAb CTC8, which was able to recognize both monomeric and oligomeric forms of CCR5, and had no neutralizing activity against CCR5-using HIV-1 (data not shown). The KG-positive and -negative subsets having the same CCR5 fluorescent intensity were then collected by fluorescent-activated cell sorter. The mean fluorescence intensities of KG in KG-positive and -negative cell fractions after sorting were 30.2 and 4.1, respectively, while mean fluorescence intensities of CCR5 were comparable (72.3 and 61.1 respectively) (Fig. 3A). The mean fluorescence intensity of CD4 was also confirmed to be comparable in KG-positive and -negative cell fractions (183 and 178, respectively). The sorted each cell fraction was then infected with HIV-1 pseudotyped with various strains of R5 Envs including JR-FL, YU-2, and Ba-L. Since the transfection of CD4-293T cells with KG-expressing vectors was possible to influence the cell condition, each cell fraction was also infected with HIV-1 pseudotyped with vesicular stomatitis virus G protein (VSV-G), which utilizes the ubiquitously expressing molecule(s) although the receptor for VSV-G remains to be confirmed (Coil and Miller, 2004; Schlegel et al., 1983). To normalize the entry efficiency of R5 HIV-1 in each fraction, we divided luciferase activities infected with R5 pseudotyped HIV-1 by those infected with VSV-G pseudotyped HIV-1. The susceptibility of CCR5+KG+ subset to R5 HIV-1 was then compared with that of CCR5+KG− subset. Although each single cell of CCR5+KG− or CCR5+KG+ subset was supposed to have oligomeric and monomeric forms of CCR5 to some extent, respectively, we found that entry efficiencies of R5 HIV-1 in CCR5+KG+ subset were always lower than those in

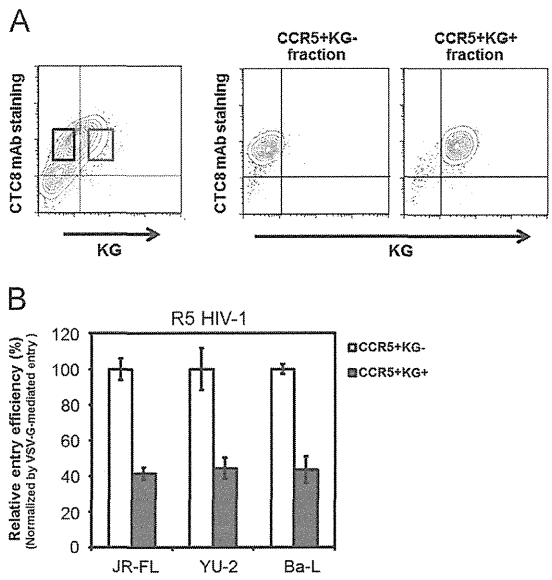

Fig. 3. Sorting of CCR5+KG− and CCR5+KG+ fractions and infection with luciferase-reporter HIV-1 pseudotyped with R5 Envs. (A) CD4-positive 293T cells expressing CCR5-KG were stained with anti-CCR5 mAb CTC8 (shown in the left panel). Representative data of flow cytometric analysis is shown. The KG− (shown in black rectangle) and KG+ (shown in gray rectangle) fractions with the same mean fluorescence intensities of CCR5 were gated, and sorted by fluorescent-activated cell sorter. Each sorted fraction was analyzed using flow cytometry (shown in the right panel). (B) Each sorted fraction was infected with luciferase-reporter HIV-1 pseudotyped with R5 Envs or VSV-G, and luciferase activities of infected cells were determined 24 h post-infection. Entry efficiency of each R5 Env in each fraction was normalized by that of VSV-G. Relative entry efficiency of CCR5+KG+ fraction (shown in gray bar) was expressed as the percentage of that of CCR5+KG− fraction (shown in white bar). The data are expressed as means ± standard deviations in triplicate experiments.

CCR5+KG− subset (Fig. 3B). These results indicated that R5 Envs preferentially recognized monomeric forms of CCR5 rather than its oligomeric forms.

Infection of KG-positive and -negative cell fractions with R5X4 HIV-1

We next checked the susceptibilities of CCR5+KG− and CCR5+KG+ subsets to another CCR5-using HIV-1, R5X4. As we mentioned earlier, there were several phenotypes in the strains of R5X4 HIV-1 such as dual-R5 and dual-X4 (Symons et al., 2011; Toma et al., 2010). We then selected 89.6 as dual-X4, KMT, TIK, and 89.6R308S as dual-R5 as previously described (Maeda et al., 2008). Similar to R5 HIV-1, dual-R5 preferentially infected CCR5+KG− fraction compared to CCR5+KG+ fraction (Fig. 4). Notably, single mutation in 11th position of the V3 loop in 89.6 (89.6R308S), which changed viral phenotype from dual-X4 to dual-R5 (Maeda et al., 2008), also significantly infected CCR5+KG− fraction than CCR5+KG+ fraction. In contrast, wild type 89.6 (dual-X4) comparably infected both CCR5+KG− and CCR5+KG+ fractions. These results indicated that dual-R5 but not dual-X4 HIV-1 also preferentially recognized monomeric CCR5 for the entry.

Infection of CCR5-KG-positive and -negative cell fractions with MVC-resistant HIV-1

Since the CCR5 antagonist MVC strongly enhanced CCR5 oligomerization in 293T cells as shown in Figs. 1 and 2, MVC-resistant HIV-1 seemed to evolve to use oligomeric forms of CCR5 for the entry. In general, MVC-resistant HIV-1s were shown to recognize MVC-bound form of CCR5 to reduce sensitivity to MVC as previously described by others and us (Kuhmann et al., 2004; Maeda et al., 2011;

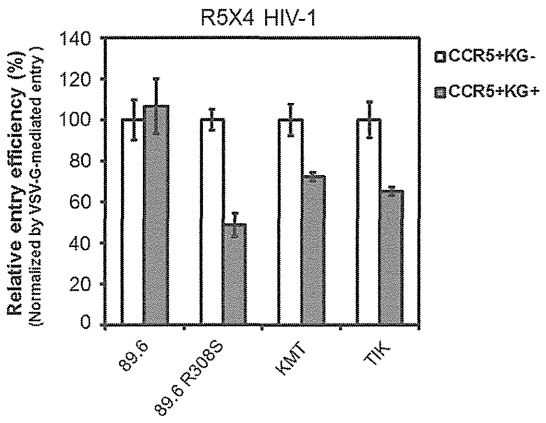

Fig. 4. Infection of CCR5+KG− and CCR5+KG+ fractions with luciferase-reporter HIV-1 pseudotyped with R5X4 Envs. Sorted CCR5+KG− and CCR5+KG+ fractions were infected with luciferase-reporter HIV-1 pseudotyped with R5X4 Envs or VSV-G. The luciferase activities of infected cells were determined 24 h post-infection. Entry efficiency of each R5X4 Env in each fraction was normalized by that of VSV-G. Relative entry efficiency of CCR5+KG+ fraction (shown in gray bar) was expressed as the percentage of that of CCR5+KG− fraction (shown in white bar). The data are expressed as means ± standard deviations in triplicate experiments.

Pugach et al., 2007; Trkola et al., 2002; Westby et al., 2007; Yuan et al., 2011). We therefore sought to infect CCR5+KG− and CCR5+KG+ fractions with MVC-resistant HIV-1 in the absence or presence of 2 μM MVC, respectively. Similar to general R5 HIV-1s, MVC-resistant HIV-1 also preferentially infected CCR5+KG− fraction in both the absence and presence of MVC compared with CCR5+KG+ fraction (Fig. 5A). We further infected both fractions at various concentrations of MVC ranging from 100 nM to 10 μM in order to check whether MVC-resistant HIV-1 recognizes MVC-bound forms of CCR5. Both fractions were also infected with MVC-sensitive HIV-1 carrying JR-FL Env to check whether sensitivity of general R5 HIV-1 to MVC is different between them. We found that MVC-sensitive HIV-1 had reduced sensitivity to MVC in CCR5+KG− fraction compared with CCR5+KG+ fraction (Fig. 5B), supporting the preferential recognition of CCR5 monomer by CCR5-using Env. We further observed reduced maximal inhibition of MVC-resistant HIV-1 in CCR5+KG− fraction compared with CCR5+KG+ fraction (Fig. 5B). These results indicated that MVC-resistant HIV-1 was likely to use MVC-bound forms of CCR5 monomer though MVC augmented CCR5 oligomerization.

Discussion

HIV-1 coreceptors CCR5 and CXCR4 are members of the seven transmembrane (7-TM) G protein-coupled receptors (GPCRs) superfamily. Recent data have shown that many GPCRs including chemokine receptors function as dimers or higher-order oligomers. To assess the formation of dimerization/oligomerization of GPCRs, fluorescent- or bioluminescent-based techniques have been applied such as BiFC, fluorescence resonance energy transfer (FRET), bioluminescence resonance energy transfer (BRET) assay (reviewed in (Vidi et al., 2011)). In the case of BiFC, the expression vectors for BiFC are generally comprised of two fragments of non-functional fluorescent protein split by N- and C-terminus (KGN and KGC of Kusabira–Green: KG in our case). When GPCRs fused to KGN and KGC are brought in close proximity, fluorescent signal can be detected by refolding of the fluorescent protein, KG. It should be noted that KG-signal could be only detected when KGN and KGC are brought together but not the same pairs such as KGN–KGN or KGC–KGC. Nonetheless, we were able to show KG-positive cells in both CCR5-KGN and CCR5-KGC expressing cells

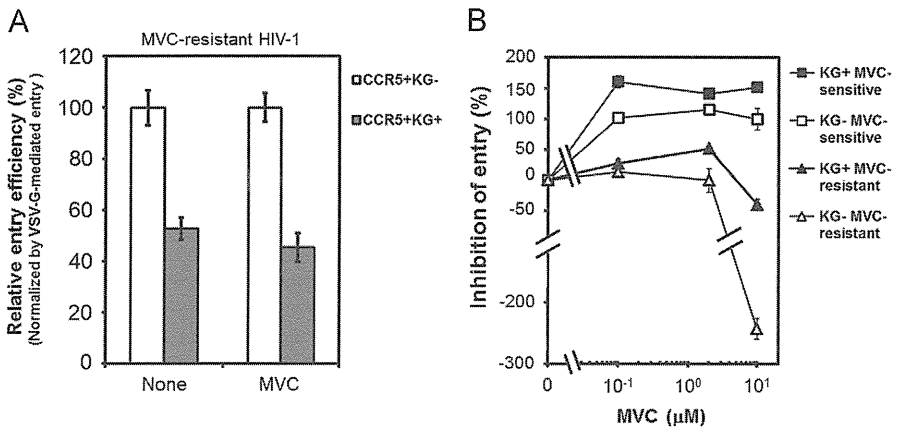

Fig. 5. Infection of CCR5+KG− and CCR5+KG+ fractions with luciferase-reporter HIV-1 pseudotyped with JR-FL and MVC-resistant Envs. (A) Sorted CCR5+KG− and CCR5+KG+ fractions were infected with luciferase-reporter HIV-1 pseudotyped with MVC-resistant Env or VSV-G in the absence or presence of 2 μM MVC. The luciferase activities of infected cells were determined 24 h post-infection. Entry efficiencies of MVC-resistant Env in CCR5+KG− and CCR5+KG+ fractions in the presence or absence of MVC were normalized by those of VSV-G, respectively. Relative entry efficiency of CCR5+KG+ fraction (shown in gray bar) was expressed as the percentage of that of CCR5+KG− fraction (shown in white bar). (B) Percentages of inhibition of MVC-sensitive (JR-FL) and MVC-resistant HIV-1s are expressed as relative values, with that of MVC-sensitive HIV-1 in CCR5+KG− fractions at 10 μM MVC being 100%. The data are expressed as means ± standard deviations in triplicate experiments.

(Fig. 1) without ligands, which were further increased by the CCR5 antagonists but not by the CXCR4 antagonist (Figs. 1 and 2). These results indicated that CCR5 was able to form dimer/oligomers. It is well known that CXCR4 exists as constitutive higher order oligomers without natural ligands (Supplementary Fig. S1) (Babcock et al., 2003; Hamatake et al., 2009; Issafras et al., 2002; Percherancier et al., 2005; Toth et al., 2004; Wu et al., 2010). CCR5 could also exist as dimer or higher order oligomers as recently described (Babcock et al., 2003; Benkirane et al., 1997; Issafras et al., 2002), although to a lesser extent than CXCR4. On the present study, we further showed not only the existence of CCR5 monomer/dimer forms without its ligands but also the enhanced oligomerization by the antagonists (Fig. 2 and Fig. S1). It has been shown that natural ligands for CCR5 such as CCL5 (RANTES) or CCL4 (MIP-1β) have been shown to induce homo-oligomerization of CCR5 (Chelli and Alizon, 2002; Hernanz-Falcon et al., 2004; Rodriguez-Frade et al., 1999; Vila-Coro et al., 2000), though its physiological role remains to be determined. Similarly, CXCR4's natural ligand SDF-1 also induced homo-dimerization of CXCR4 as previously described (Percherancier et al., 2005; Toth et al., 2004; Vila-Coro et al., 1999). In contrast, oligomerization of chemokine receptors by their antagonists has not been described to date though another GPCR melatonin receptor was reported to form dimer by both agonists and antagonists (Ayoub et al., 2002). The dimerization of melatonin receptor by both agonist and antagonists was explained by the stabilization of its conformations. Interestingly, in the presence of MVC, CCR5+KG+ subset became well detected by the anti-CCR5 mAb recognizing the conformational epitope (clone 45549) (Fig. 1), indicating that conformations of CCR5 induced by MVC might be also structurally stable. In our flow cytometric analyses without addition of ligands, CCR5+KG+ subsets were equally detected by most anti-CCR5 mAbs except the clone 45549 (Fig. 1). Given that several antigenic conformations of CCR5 existed on the cell surface (Berro et al., 2011; Lee et al., 1999), oligomer forms of CCR5 might have the similar antigenic conformations while monomeric forms had different antigenic conformations.

Previous reports have shown that several GPCRs were homo- or hetero-oligomerized in endoplasmic reticulum (ER) (Herrick-Davis et al., 2006; Issafras et al., 2002; Milligan, 2010; Salahpour et al., 2004; Vischer et al., 2011). In our BiFC assay using confocal laser scanning microscopy, CCR5-KG signals were also detected not only at plasma membrane but also in intracellular compartments, both of which were further enhanced by the addition of MVC (Fig. 2E). Time-course experiments also showed that more than 24 h were needed for the enhanced oligomerization of CCR5 by MVC (Fig. 2D). These findings suggested that oligomerization of CCR5 were formed during early biosynthesis and protein maturation in the ER, and that MVC may further enhance CCR5 oligomerization by the binding of intracellular CCR5. Thus, it is possible that MVC could penetrate into the cell membrane and act before the expression of CCR5 on the cell surface. It is of note that the concentration to induce oligomerization of CCR5 was sufficiently low similar to the concentration that is able to inhibit R5 HIV-1 replication (Fig. 2C), indicating the concentrations of MVC, which would be achieved in HIV-1-infected individuals treated with MVC, seems to induce oligomerization of CCR5 to some extent *in vivo*, although the pharmacological and pathological roles of MVC-induced CCR5 oligomerization in primary T cells and macrophages still remains to be determined.

As we mentioned above, it is possible that CCR5 monomer may have multiple forms, whereas the oligomers may have relatively fixed forms. Since R5 HIV-1 is supposed to recognize specific forms of CCR5 (Berro et al., 2011, 2013), we attempted to check which form of CCR5, monomer or oligomer, is used by R5 HIV-1. To this end, CCR5+KG− and CCR5+KG+ subsets expressed in CD4-positive 293T cells were fractionated by fluorescent-activated cell sorter, and infected with pseudotyped R5 HIV-1. The CCR5+KG− and CCR5+KG+ subsets could have relatively lower and higher amount of oligomeric forms, respectively, while both CCR5+KG− and CCR5+KG+ subsets are supposed to have monomeric and oligomeric forms of CCR5 in flow cytometry analysis. Nevertheless, we were able to show that CCR5+KG+fraction was less susceptible to R5 and dual-R5 HIV-1 than CCR5+KG− fraction (Fig. 3 and 4). It is thus likely that R5 and dual-R5 Envs preferentially recognized monomeric forms of CCR5. The dimerization induced by the monoclonal antibody CCR5-02 was previously reported to cause blocking of HIV-1 entry (Vila-Coro et al., 2000). Our present study further clarified that the oligomerization of CCR5 without ligands also affected the susceptibility to R5 and dual-R5 HIV-1.

Although the susceptibility of KG-negative cell fraction to R5 and dual-R5 HIV-1 was significantly high, dual-X4 HIV-1 89.6 equally infected both CCR5+KG− and CCR5+KG+ fraction (Fig. 4). It is therefore possible that dual-X4 lost the preferential recognition of monomeric forms of CCR5, and may commence recognizing homo-oligomeric forms of CCR5. Intriguingly, the single mutation in 89.6 from arginine to serine at 11th position of the V3 loop (89.6R308S), which changed the tropism from dual-X4 to dual-R5 (Maeda et al.,

2008), also reverted to recognize monomeric forms of CCR5. Hence, the single amino acid substitution was sufficient to lose preferential recognition of monomer forms of CCR5 for CCR5-using HIV-1.

As described by others and us, MVC-resistant HIV-1 recognized MVC-bound and -unbound forms of CCR5 (Kuhmann et al., 2004; Maeda et al., 2011; Pugach et al., 2007; Trkola et al., 2002; Westby et al., 2007; Yuan et al., 2011). Since MVC was found to enhance CCR5 oligomerization in our present study, we then sought to check whether MVC-resistant HIV-1 recognizes MVC-bound forms of CCR5 oligomers. However, similar to R5 HIV-1, we found that MVC-resistant HIV-1 recognized both MVC-bound and -unbound forms of CCR5 monomer (Fig. 5). Since numbers of MVC-bound forms of CCR5 monomer would be dependent on the surface expression levels of CCR5 and cell types, our findings may partly explain why susceptibility to CCR5 antagonists was dependent on the cell types as previously described (Berro et al., 2011). Taken together, it is likely that R5 HIV-1 including MVC-resistant HIV-1 constrained to use monomeric forms of CCR5 for the entry.

In conclusion, we were able to show that oligomeric forms of CCR5 were less susceptible to R5 HIV-1 than the monomeric forms. However, our findings were obtained from the cells expressing high levels of CCR5 *in vitro*. Therefore, it is quite important to understand the role of CCR5 oligomerization in primary T cells and macrophages for HIV-1 entry *in vivo*. The methods to detect native forms of homo- and hetero-oligomerized CCR5 and their susceptibilities to HIV-1 in primary cells should be established and analyzed to elucidate the role of CCR5 oligomerization for HIV-1 infection *in vivo*.

Materials and methods

Cells and culture conditions

The 293T and HeLa cells were maintained in Dulbecco's modified Eagle medium (DMEM) (Sigma-Aldrich) supplemented with 10% fetal bovine serum (FBS) (Gibco BRL), 100 U/ml of penicillin and 100 μg/ml of streptomycin. A human CD4-expressing glioma cell line (NP2/CD4) was maintained in Eagle's minimum essential medium (MEM; Gibco BRL) supplemented with 10% FBS, 100 U/ml of penicillin and 100 μg/ml of streptomycin (Jinno et al., 1998).

Coreceptor antagonists

A CXCR4 antagonist AMD3100 (Schols et al., 1997a, 1997b) and a CCR5 antagonist maraviroc (MVC) (Dorr et al., 2005) were supplied by the AIDS Research and Reference Reagent Program, Division of AIDS, National Institute of Allergy and Infectious Diseases. A CCR5 antagonist TAK-779 (Baba et al., 1999) was kindly obtained from Takeda Chemical Industries (Osaka, Japan).

Construction of retrovirus vector and transduction of 293T cells with the CD4 gene

The cDNA encoding human CD4 was obtained by PCR using human lymphocyte cDNA as the template. The primers used were as follows: 5′-CTCGAGTCGCCACCATGAACCGGGGAGTCCCTTTTAGC-3′ and 5′-TCAAATGGGGCTACATGTCTTCTGAAACCG-3′ (underlined are *Xho*I site). The amplified product was cloned into pCR-TOPO (Invitrogen), and the sequence was verified using 3130 Genetic Analyzer (Applied Biosystems). A CCR5 carrying *Xho*I-*Eco*RI fragments was ligated into pMSCVpuro (Clothech) to generate pMSCVpuro-CD4. Retrovirus vector was produced according to the manufacturer's instructions, and 293T cells were then transduced and selected by puromycin (Sigma-Aldrich). The CD4 expression of the transduced 293T cells was verified by anti-CD4 monoclonal antibody (RPA-T4, eBioscience).

Expression vectors

CCR5 expression vectors for BiFC was constructed using phmKGN-MN and phmKGC-MN (MBL, Japan) according to the manufacture's instructions. Briefly, human CCR5 gene was amplified using pCR2-CCR5 as a template (Maeda et al., 2000). Primers used were: 5′-CTCGAGGAACAAGATGGATTATCAAGTG-3′ and 5′-GTCTAGATTACT TGTCGTCATCGTCTTTGTAGTCCAAGCCCACAGATA-3′ (underlined are *Xho*I and *Xba*I restriction enzyme sites, respectively). The amplified product was cloned into pCR-TOPO, and the sequence was verified using 3130 Genetic Analyzer. The *Xho*I-*Xba*I fragment carrying CCR5 gene was then ligated into both phmKGN-MN and phmKGC-MN using *Xho*I and *Xba*I sites to generate pCCR5-KGN and pCCR5-KGC respectively. To construct an expression vector of FLAG-tagged CCR5, CCR5 sequence was amplified using primer: 5′-CTCGAGGAACAAGATGGAT-TATCAAGTG-3′ and 5′-GTCTAGATTACTTGTCGTCATCGTCTTTGTAGTC-CAAGCCCACAGATAT-3′ (underlined are the *Xho*I and *Xba*I restriction enzyme sites, respectively). The amplified product was cloned into pCR-TOPO, and the sequence was then verified using a 3130 Genetic Analyzer. The amplified fragment was finally ligated into phmKGC-MN expression vector (In this vector, split fluorescence protein, Kusabira–Green: KG, was replaced with FLAG-tag by digestion of the *Xho*I and *Xba*I restriction enzyme sites). Expression vectors for JR-FL, 89.6, 89.6R308S, KMT and TIK Envs were prepared as previously described (Maeda et al., 2000, 2008). Expression vectors for Ba-L and YU-2 Envs were kindly supplied by K. Yoshimura (National Institute of Infectious diseases, Tokyo). An expression vector for MVC-resistant Env was prepared as previously described (Yuan et al., 2011, 2013).

Production of recombinant luciferase-reporter virus

Recombinant luciferase-reporter virus of pseudotyped with various HIV-1 Envs or VSV-G were produced by transfection of 293T cells using the calcium phosphate method (ProFection Mammalian Transfection System, Promega) as previously described (Maeda et al., 2000, 2008). The cells culture supernatant was collected 48 h post-transfection, filtered with 0.45 μm pore-size, and stocked at −80 °C until use. The p24 Gag in the culture supernatant was measured using HIV-1 p24 Ag ELISA kit (Zeptometrix) according to manufacture's instructions.

Detection of the CCR5 expression in KG-positive and -negative cell population

The 293T cells were transfected with CCR5-KG expression vectors, pCCR5-KGN and pCCR5-KGC, using calcium phosphate method, and incubated for 48 h or indicated time of period at 37 °C in the presence or absence of 2 μM of AMD3100, TAK-779 or MVC. In a dose-escalating study, transfected cells were treated with various concentrations of MVC (ranging from 0.0002 μM to 2 μM) for 48 h. To detect the CCR5 in CCR5-KG-transfected cells, the cells were first incubated with anti-CCR5 mAbs, 3A9, CTC8, 45531, 45549 (R&D Systems), or 2D7 (BD Pharmingen) for 30 min at 4 °C. The cells were then stained with β-phycoerythrin-conjugated anti-mouse IgG antibody (Jackson Immuno Research). For direct detection of the CCR5 expression in CCR5-KG-transfected cells, the cells were stained with anti-human CCR5 mAb 2D7 conjugated with Alexa Fluor 647 (BioLegend) for 30 min at 4 °C. The cells were analyzed by FACScan or FACSCalibur fluorescent-activated cell sorter (Becton Dickinson).

Detection of monomeric and oligomeric forms of CCR5 by Western blot

The transfected 293T cells with pCCR5-FLAG expression vector were incubated at 37 °C for 48 h with or without MVC. The cells were treated with DSP (dithiobis[succinimidylpropionate]) cross-linker according to the manufacture's instructions (Thermo Scientific), and solubilized using 1% Brij O10 (Sigma-Aldrich) lysis buffer (1% Brij O10, 20 mM Tris–HCl pH 8.2, 0.15 M NaCl, 5 mM iodoacetamide) including protease inhibitor cocktail (Sigma-Aldrich). The cell lysates were then separated by SDS-PAGE, blotted onto PVDF (polyvinylidene fluoride, Immobilon-P, Millipore) membrane. The membranes were incubated with anti-FLAG mAb (Wako) or anti-β-actin mAb (Sigma-Aldrich) for 90 min, followed by staining with horseradish peroxidase (HRP)-conjugated anti-mouse IgG (Jackson Immuno Research). The signals were detected using Chemi-Lumi One (Nacalai Tesque).

Confocal laser scanning microscopy

The HeLa cells were plated to collagen (Atelo Cell)-coated 8-well glass slides (Lab-Tek). The cells were transfected with both pCCR5-KGN and pCCR5-KGC using Lipofectamine 2000 (Invitrogen) according to the manufacture's instructions. Transfected cells were incubated at 37 °C for 48 h in the presence or absence of 1 μM MVC. The cells were fixed with 4% paraformaldehyde (Wako) for 15 min, and analyzed using LSM-700-ZEN confocal laser scanning microscopy (Carl Zeiss) with a 60X objective lens. The images were processed using LSM Imaging Browser (Carl Zeiss).

Fluorescence-activated cell sorting of CCR5-KG-positive and -negative cell fraction and infection with pseudotyped HIV-1

The CD4-293T cells were transfected with pCCR5-KGN and pCCR5-KGC using calcium phosphate method. After 48 h cultures at 37 °C, cells were stained with anti-CCR5 mAb CTC8, followed by staining with APC-conjugated anti-mouse IgG. The cells were then sorted into CCR5+KG− and CCR5+KG+ fractions with the same expression levels of CCR5 by using FACS AriaII (Becton Dickinson) according to the manufacture's instructions. Sorted each fraction was then incubated with the same amount (40 ng of p24Ag) of luciferase-reporter HIV-1 pseudotyped with various HIV-1 Envs including R5 (JR-FL, YU-2, Ba-L), R5X4 (89.6 wt, 89.6 R308S (Maeda et al., 2008), KMT, and TIK), MVC-resistant Env (T199K/T275M/V3-M5) (Yuan et al., 2011, 2013) or VSV-G at 37 °C for 30 min to allow adsorption of the virus. The cells were washed to remove unadsorbed virus, seeded into a 96-well plate, and cultured at 37 °C for 24 h. Luciferase activity was measured using a luminometer, Lumat LB 9501/16 (EG&G Berthold, Bad Wildbad). The entry efficiency of HIV-1 infected by HIV-1 Envs in each cell fraction was normalized by the luciferase activity of the same fraction infected by VSV-G.

Acknowledgments

We thank Dr. Kazuhisa Yoshimura and Takeda Chemical Industries for providing Env expression vectors of YU-2 and Ba-L, and TAK-779, respectively. Thanks are also due to Dr. Kazuhisa Yoshimura and Dr. Shuzo Matsushita for helpful discussions. This work was supported by Grants-in-Aid for Scientific Research, and the Global COE program "Global Education and Research Center Aiming at the control of AIDS" supported by the Ministry of Education, Science, Sports, and Culture of Japan; by a Grant-in-Aid for scientific research from the Ministry of Health of Japan.

Appendix A. Supplementary material

Supplementary data associated with this article can be found in the online version at http://dx.doi.org/10.1016/j.virol.2013.12.034.

References

Alkhatib, G., Locati, M., Kennedy, P.E., Murphy, P.M., Berger, E.A., 1997. HIV-1 coreceptor activity of CCR5 and its inhibition by chemokines: independence from G protein signaling and importance of coreceptor downmodulation. Virology 234, 340–348.

Ayoub, M.A., Couturier, C., Lucas-Meunier, E., Angers, S., Fossier, P., Bouvier, M., Jockers, R., 2002. Monitoring of ligand-independent dimerization and ligand-induced conformational changes of melatonin receptors in living cells by bioluminescence resonance energy transfer. J. Biol. Chem. 277, 21522–21528.

Baba, M., Nishimura, O., Kanzaki, N., Okamoto, M., Sawada, H., Iizawa, Y., Shiraishi, M., Aramaki, Y., Okonogi, K., Ogawa, Y., Meguro, K., Fujino, M., 1999. A small-molecule, nonpeptide CCR5 antagonist with highly potent and selective anti-HIV-1 activity. Proc. Nat. Acad. Sci. U.S.A. 96, 5698–5703.

Babcock, G.J., Farzan, M., Sodroski, J., 2003. Ligand-independent dimerization of CXCR4, a principal HIV-1 coreceptor. J. Biol. Chem. 278, 3378–3385.

Benkirane, M., Jin, D.-Y., Chun, R.F., Koup, R.A., Jeang, K.-T., 1997. Mechanism of transdominant inhibition of CCR5-mediated HIV-1 infection by ccr5Δ32. J. Biol. Chem. 272, 30603–30606.

Berro, R., Klasse, P.J., Lascano, D., Flegler, A., Nagashima, K.A., Sanders, R.W., Sakmar, T.P., Hope, T.J., Moore, J.P., 2011. Multiple CCR5 conformations on the cell surface are used differentially by human immunodeficiency viruses resistant or sensitive to CCR5 inhibitors. J. Virol. 85, 8227–8240.

Berro, R., Yasmeen, A., Abrol, R., Trzaskowski, B., Abi-Habib, S., Grunbeck, A., Lascano, D., Goddard, W.A., Klasse, P.J., Sakmar, T.P., Moore, J.P., 2013. Use of G-protein-coupled and -uncoupled CCR5 receptors by CCR5 inhibitor-resistant and -sensitive human immunodeficiency virus type 1 variants. J. Virol. 87, 6569–6581.

Chelli, M., Alizon, M., 2002. Rescue of HIV-1 receptor function through cooperation between different forms of the CCR5 chemokine receptor. J. Biol. Chem. 277, 39388–39396.

Cocchi, F., DeVico, A.L., Garzino-Demo, A., Arya, S.K., Gallo, R.C., Lusso, P., 1995. Identification of RANTES, MIP-1 alpha, and MIP-1 beta as the major HIV-suppressive factors produced by CD8+ T cells. Science 270, 1811–1815.

Coil, D.A., Miller, A.D., 2004. Phosphatidylserine is not the cell surface receptor for vesicular stomatitis virus. J. Virol. 78, 10920–10926.

Connor, R.I., Sheridan, K.E., Ceradini, D., Choe, S., Landau, N.R., 1997. Change in coreceptor use correlates with disease progression in HIV-1-infected individuals. J. Exp. Med. 185, 621–628.

Dorr, P., Westby, M., Dobbs, S., Griffin, P., Irvine, B., Macartney, M., Mori, J., Rickett, G., Smith-Burchnell, C., Napier, C., Webster, R., Armour, D., Price, D., Stammen, B., Wood, A., Perros, M., 2005. Maraviroc (UK-r27,857), a potent, orally bioavailable, and selective small-molecule inhibitor of chemokine receptor CCR5 with broad-spectrum anti-human immunodeficiency virus type 1 activity. Antimicrob. Agents Chemother. 49, 4721–4732.

Dragic, T., Trkola, A., Thompson, D.A., Cormier, E.G., Kajumo, F.A., Maxwell, E., Lin, S.W., Ying, W., Smith, S.O., Sakmar, T.P., Moore, J.P., 2000. A binding pocket for a small molecule inhibitor of HIV-1 entry within the transmembrane helices of CCR5. Proc. Nat. Acad. Sci. U.S.A. 97, 5639–5644.

El-Asmar, L., Springael, J.Y., Ballet, S., Andrieu, E.U., Vassart, G., Parmentier, M., 2005. Evidence for negative binding cooperativity within CCR5-CCR2b heterodimers. Mol. Pharmacol. 67, 460–469.

Hamatake, M., Aoki, T., Futahashi, Y., Urano, E., Yamamoto, N., Komano, J., 2009. Ligand-independent higher-order multimerization of CXCR4, a G-protein-coupled chemokine receptor involved in targeted metastasis. Cancer Sci. 100, 95–102.

Hammad, M.M., Kuang, Y.Q., Yan, R., Allen, H., Dupre, D.J., 2010. Na+/H+ exchanger regulatory factor-1 is involved in chemokine receptor homodimer CCR5 internalization and signal transduction but does not affect CXCR4 homodimer or CXCR4–CCR5 heterodimer. J. Biol. Chem. 285, 34653–34664.

Hernanz-Falcon, P., Rodriguez-Frade, J.M., Serrano, A., Juan, D., del Sol, A., Soriano, S. F., Roncal, F., Gomez, L., Valencia, A., Martinez-A, C., Mellado, M., 2004. Identification of amino acid residues crucial for chemokine receptor dimerization. Nat. Immunol. 5, 216–223.

Herrick-Davis, K., Weaver, B.A., Grinde, E., Mazurkiewicz, J.E., 2006. Serotonin 5-HT2C receptor homodimer biogenesis in the endoplasmic reticulum: real-time visualization with confocal fluorescence resonance energy transfer. J. Biol. Chem. 281, 27109–27116.

Issafras, H., Angers, S., Bulenger, S., Blanpain, C., Parmentier, M., Labbé-Jullié, C., Bouvier, M., Marullo, S., 2002. Constitutive agonist-independent CCR5 oligomerization and antibody-mediated clustering occurring at physiological levels of receptors. J. Biol. Chem. 277, 34666–34673.

Jinno, A., Shimizu, N., Soda, Y., Haraguchi, Y., Kitamura, T., Hoshino, H., 1998. Identification of the chemokine receptor TER1/CCR8 expressed in brain-derived cells and T cells as a new coreceptor for HIV-1 infection. Biochem. Biophys. Res. Commun. 243, 497–502.

Kerppola, T.K., 2008. Bimolecular fluorescence complementation (BiFC) analysis as a probe of protein interactions in living cells. Annu. Rev. Biophys. 37, 465–487.

Kondru, R., Zhang, J., Ji, C., Mirzadegan, T., Rotstein, D., Sankuratri, S., Dioszegi, M., 2008. Molecular interactions of CCR5 with major classes of small-molecule anti-HIV CCR5 antagonists. Mol. Pharmacol. 73, 789–800.

Kuhmann, S.E., Pugach, P., Kunstman, K.J., Taylor, J., Stanfield, R.L., Snyder, A., Strizki, J.M., Riley, J., Baroudy, B.M., Wilson, I.A., Korber, B.T., Wolinsky, S.M., Moore, J.P., 2004. Genetic and phenotypic analyses of human immunodeficiency virus type 1 escape from a small-molecule CCR5 Inhibitor. J. Virol. 78, 2790–2807.

Lee, B., Sharron, M., Blanpain, C., Doranz, B.J., Vakili, J., Setoh, P., Berg, E., Liu, G., Guy, H.R., Durell, S.R., Parmentier, M., Chang, C.N., Price, K., Tsang, M., Doms, R.W., 1999. Epitope mapping of CCR5 reveals multiple conformational states and distinct but overlapping structures involved in chemokine and coreceptor function. J. Biol. Chem. 274, 9617–9626.

Maeda, K., Das, D., Ogata-Aoki, H., Nakata, H., Miyakawa, T., Tojo, Y., Norman, R., Takaoka, Y., Ding, J., Arnold, G.F., Arnold, E., Mitsuya, H., 2006. Structural and molecular interactions of CCR5 inhibitors with CCR5. J. Biol. Chem. 281, 12688–12698.

Maeda, Y., Foda, M., Matsushita, S., Harada, S., 2000. Involvement of both the V2 and V3 regions of the CCR5-tropic human immunodeficiency virus type 1 envelope in reduced sensitivity to macrophage inflammatory protein 1α. J. Virol. 74, 1787–1793.

Maeda, Y., Yoshimura, K., Miyamoto, F., Kodama, E., Harada, S., Yuan, Y., Harada, S., Yusa, K., 2011. In vitro and In vivo resistance to human immunodeficiency virus type 1 entry inhibitors. AIDS Clin. Res., S2.

Maeda, Y., Yusa, K., Harada, S., 2008. Altered sensitivity of an R5X4 HIV-1 strain 89.6 to coreceptor inhibitors by a single amino acid substitution in the V3 region of gp120. Antiviral Res. 77, 128–135.

Mellado, M., Rodriguez-Frade, J.M., Vila-Coro, A.J., Fernandez, S., Martin de Ana, A., Jones, D.R., Toran, J.L., Martinez-A, C., 2001. Chemokine receptor homo- or heterodimerization activates distinct signaling pathways. EMBO J. 20, 2497–2507.

Milligan, G., 2010. The role of dimerisation in the cellular trafficking of G-protein-coupled receptors. Curr. Opin. Pharmacol. 10, 23–29.

Nishikawa, M., Takashima, K., Nishi, T., Furuta, R.A., Kanzaki, N., Yamamoto, Y., Fujisawa, J.-i., 2005. Analysis of binding sites for the new small-molecule CCR5 antagonist TAK-220 on human CCR5. Antimicrob. Agents Chemother. 49, 4708–4715.

Oberlin, E., Amara, A., Bachelerie, F., Bessia, C., Virelizier, J.L., Arenzana-Seisdedos, F., Schwartz, O., Heard, J.M., Clark-Lewis, I., Legler, D.F., Loetscher, M., Baggiolini, M., Moser, B., 1996. The CXC chemokine SDF-1 is the ligand for LESTR/fusin and prevents infection by T-cell-line-adapted HIV-1. Nature 382, 833–835.

Percherancier, Y., Berchiche, Y.A., Slight, I., Volkmer-Engert, R., Tamamura, H., Fujii, N., Bouvier, M., Heveker, N., 2005. Bioluminescence resonance energy transfer reveals ligand-induced conformational changes in CXCR4 homo- and heterodimers. J. Biol. Chem. 280, 9895–9903.

Pugach, P., Marozsan, A.J., Ketas, T.J., Landes, E.L., Moore, J.P., Kuhmann, S.E., 2007. HIV-1 clones resistant to a small molecule CCR5 inhibitor use the inhibitor-bound form of CCR5 for entry. Virology 361, 212–228.

Rodriguez-Frade, J.M., Vila-Coro, A.J., Martin, A., Nieto, M., Sanchez-Madrid, F., Proudfoot, A.E., Wells, T.N., Martinez, A.C., Mellado, M., 1999. Similarities and differences in RANTES- and (AOP)-RANTES-triggered signals: implications for chemotaxis. J. Cell Biol. 144, 755–765.

Salahpour, A., Angers, S., Mercier, J.-F., Lagacé, M., Marullo, S., Bouvier, M., 2004. Homodimerization of the β2-adrenergic receptor as a prerequisite for cell surface targeting. J. Biol. Chem. 279, 33390–33397.

Scarlatti, G., Tresoldi, E., Bjorndal, A., Fredriksson, R., Colognesi, C., Deng, H.K., Malnati, M.S., Plebani, A., Siccardi, A.G., Littman, D.R., Fenyo, E.M., Lusso, P., 1997. In vivo evolution of HIV-1 co-receptor usage and sensitivity to chemokine-mediated suppression. Nat. Med. 3, 1259–1265.

Schlegel, R., Tralka, T.S., Willingham, M.C., Pastan, I., 1983. Inhibition of VSV binding and infectivity by phosphatidylserine: is phosphatidylserine a VSV-binding site? Cell 32, 639–646.

Schols, D., Este, J.A., Henson, G., De Clercq, E., 1997a. Bicyclams, a class of potent anti-HIV agents, are targeted at the HIV coreceptor fusin/CXCR-4. Antiviral Res. 35, 147–156.

Schols, D., Struyf, S., Van Damme, J., Este, J.A., Henson, G., De Clercq, E., 1997b. Inhibition of T-tropic HIV strains by selective antagonization of the chemokine receptor CXCR4. J. Exp. Med. 186, 1383–1388.

Seibert, C., Ying, W., Gavrilov, S., Tsamis, F., Kuhmann, S.E., Palani, A., Tagat, J.R., Clader, J.W., McCombie, S.W., Baroudy, B.M., Smith, S.O., Dragic, T., Moore, J.P., Sakmar, T.P., 2006. Interaction of small molecule inhibitors of HIV-1 entry with CCR5. Virology 349, 41–54.

Sohy, D., Yano, H., de Nadai, P., Urizar, E., Guillabert, A., Javitch, J.A., Parmentier, M., Springael, J.-Y., 2009. Hetero-oligomerization of CCR2, CCR5, and CXCR4 and the protean effects of "selective" antagonists. J. Biol. Chem. 284, 31270–31279.

Symons, J., van Lelyveld, S.F., Hoepelman, A.I., van Ham, P.M., de Jong, D., Wensing, A.M., Nijhuis, M., 2011. Maraviroc is able to inhibit dual-R5 viruses in a dual/mixed HIV-1-infected patient. J. Antimicrob. Chemother. 66, 890–895.

Toma, J., Whitcomb, J.M., Petropoulos, C.J., Huang, W., 2010. Dual-tropic HIV type 1 isolates vary dramatically in their utilization of CCR5 and CXCR4 coreceptors. AIDS 24, 2181–2186.

Toth, P.T., Ren, D., Miller, R.J., 2004. Regulation of CXCR4 receptor dimerization by the chemokine SDF-1alpha and the HIV-1 coat protein gp120: a fluorescence resonance energy transfer (FRET) study. J. Pharmacol. Exp. Ther. 310, 8–17.

Trkola, A., Kuhmann, S.E., Strizki, J.M., Maxwell, E., Ketas, T., Morgan, T., Pugach, P., Xu, S., Wojcik, L., Tagat, J., Palani, A., Shapiro, S., Clader, J.W., McCombie, S., Reyes, G.R., Baroudy, B.M., Moore, J.P., 2002. HIV-1 escape from a small molecule, CCR5-specific entry inhibitor does not involve CXCR4 use. Proc. Nat. Acad. Sci. U.S.A. 99, 395–400.

Tsamis, F., Gavrilov, S., Kajumo, F., Seibert, C., Kuhmann, S., Ketas, T., Trkola, A., Palani, A., Clader, J.W., Tagat, J.R., McCombie, S., Baroudy, B., Moore, J.P., Sakmar, T.P., Dragic, T., 2003. Analysis of the mechanism by which the small-molecule CCR5 antagonists SCH-351125 and SCH-350581 inhibit human immunodeficiency virus type 1 entry. J. Virol. 77, 5201–5208.

Vidi, P.-A., Ejendal, K.F.K., Przybyla, J.A., Watts, V.J., 2011. Fluorescent protein complementation assays: new tools to study G protein-coupled receptor oligomerization and GPCR-mediated signaling. Mol. Cell. Endocrinol. 331, 185–193.

Vila-Coro, A.J., Mellado, M., Martín de Ana, A., Lucas, P., del Real, G., Martínez-A., C., Rodríguez-Frade, J.M, 2000. HIV-1 infection through the CCR5 receptor is blocked by receptor dimerization. Proc. Nat. Acad. Sci. U.S.A. 97, 3388–3393.

Vila-Coro, A.J., Rodriguez-Frade, J.M., Martin De Ana, A., Moreno-Ortiz, M.C., Martinez, A.C., Mellado, M., 1999. The chemokine SDF-1alpha triggers CXCR4 receptor dimerization and activates the JAK/STAT pathway. FASEB J. 13, 1699–1710.

Vischer, H.F., Watts, A.O., Nijmeijer, S., Leurs, R., 2011. G protein-coupled receptors: walking hand-in-hand, talking hand-in-hand? Br. J. Pharmacol. 163, 246–260.

Westby, M., Smith-Burchnell, C., Mori, J., Lewis, M., Mosley, M., Stockdale, M., Dorr, P., Ciaramella, G., Perros, M., 2007. Reduced maximal inhibition in phenotypic susceptibility assays indicates that viral strains resistant to the CCR5 antagonist maraviroc utilize inhibitor-bound receptor for entry. J. Virol. 81, 2359–2371.

Wilen, C.B., Tilton, J.C., Doms, R.W., 2012. HIV: cell binding and entry. Cold Spring Harb. Perspect. Med., 2.

Wu, B., Chien, E.Y.T., Mol, C.D., Fenalti, G., Liu, W., Katritch, V., Abagyan, R., Brooun, A., Wells, P., Bi, F.C., Hamel, D.J., Kuhn, P., Handel, T.M., Cherezov, V., Stevens, R.C., 2010. Structures of the CXCR4 chemokine GPCR with small-molecule and cyclic peptide antagonists. Science 330, 1066–1071.

Yuan, Y., Maeda, Y., Terasawa, H., Monde, K., Harada, S., Yusa, K., 2011. A combination of polymorphic mutations in V3 loop of HIV-1 gp120 can confer noncompetitive resistance to maraviroc. Virology 413, 293–299.

Yuan, Y., Yokoyama, M., Maeda, Y., Terasawa, H., Harada, S., Sato, H., Yusa, K., 2013. Structure and dynamics of the gp120 V3 loop that confers noncompetitive resistance in R5 HIV-1_{JR-FL} to maraviroc. PLoS One 8, e65115.

PLOS ONE

V3-Independent Competitive Resistance of a Dual-X4 HIV-1 to the CXCR4 Inhibitor AMD3100

Yosuke Maeda[1]*, Hiromi Terasawa[1], Yusuke Nakano[1], Kazuaki Monde[1], Keisuke Yusa[2], Shinichi Oka[3], Masafumi Takiguchi[4], Shinji Harada[1]

1 Department of Medical Virology, Faculty of Life Sciences, Kumamoto University, Kumamoto, Japan, **2** Division of Biological Chemistry and Biologicals, National Institute of Health Sciences, Tokyo, Japan, **3** AIDS Clinical Center, National Center for Global Health and Medicine, Tokyo, Japan, **4** Center for AIDS Research, Kumamoto University, Kumamoto, Japan

Abstract

A CXCR4 inhibitor-resistant HIV-1 was isolated from a dual-X4 HIV-1 *in vitro*. The resistant variant displayed competitive resistance to the CXCR4 inhibitor AMD3100, indicating that the resistant variant had a higher affinity for CXCR4 than that of the wild-type HIV-1. Amino acid sequence analyses revealed that the resistant variant harbored amino acid substitutions in the V2, C2, and C4 regions, but no remarkable changes in the V3 loop. Site-directed mutagenesis confirmed that the changes in the C2 and C4 regions were principally involved in the reduced sensitivity to AMD3100. Furthermore, the change in the C4 region was associated with increased sensitivity to soluble CD4, and profoundly enhanced the entry efficiency of the virus. Therefore, it is likely that the resistant variant acquired the higher affinity for CD4/CXCR4 by the changes in non-V3 regions. Taken together, a CXCR4 inhibitor-resistant HIV-1 can evolve using a non-V3 pathway.

Citation: Maeda Y, Terasawa H, Nakano Y, Monde K, Yusa K, et al. (2014) V3-Independent Competitive Resistance of a Dual-X4 HIV-1 to the CXCR4 Inhibitor AMD3100. PLoS ONE 9(2): e89515. doi:10.1371/journal.pone.0089515

Editor: Luis Menéndez-Arias, Centro de Biología Molecular Severo Ochoa (CSIC-UAM), Spain

Received November 26, 2013; **Accepted** January 23, 2014; **Published** February 19, 2014

Funding: This work was supported by a Joint Research Grant from the Institute of Tropical Medicine, Nagasaki University, and the Global COE program "Global Education and Research Center Aiming at the control of AIDS" supported by the Ministry of Education, Culture, Sports, Science and Technology of Japan. The funders had no role in study design, data collection and analysis, decision to publish, or preparation of the manuscript.

Competing Interests: The authors have declared that no competing interests exist.

* E-mail: ymaeda@kumamoto-u.ac.jp

Introduction

The entry of human immunodeficiency virus type 1 (HIV-1) is initiated by an interaction of viral envelope glycoprotein gp120 with the principal receptor CD4 and one of the coreceptors, either CCR5 or CXCR4, expressed in the target cells. HIV-1 is classified into three phenotypes based on its ability to use CCR5 (R5), CXCR4 (X4), or both (R5X4 or dual-tropic). Certain dual-tropic viruses are further classified into those that prefer CCR5 (dual-R5) or CXCR4 (dual-X4) [1,2]. It has been shown that the coreceptor usage of HIV-1 is mainly determined by the third variable region of gp120 (V3 loop) [3,4,5] that is composed of ~35 amino acids. In particular, the number and position of positively charged amino acids in the V3 loop are important for coreceptor selectivity such as the 11/25 rule. If the 11th or 25th positions of the V3 loop are positively charged, viruses will use CXCR4. Otherwise, they will use CCR5 [6]. Lack of an N-linked glycan at the 6th position of the V3 loop is also involved in CXCR4 usage [7,8,9]. In general, R5 viruses are predominant in the early stage of infection, whereas CXCR4-using viruses (dual-tropic and X4 viruses) emerge at the late stage of infection and are associated with disease progression in half of HIV-1-infected individuals [10,11,12]. It has been postulated that coreceptor inhibitors or natural ligands of CCR5 or CXCR4 might induce the coreceptor shift of HIV-1 between CCR5 and CXCR4. However, *in vitro* studies have shown that these escape variants acquired resistance using the same coreceptor. For example, MIP-1α (a natural ligand for CCR5)-induced escape variants of R5 HIV-1 and selected viruses exhibit substitutions in the V2 region and V3 loop without changing CCR5 usage of the virus [13]. CCR5 inhibitors such as maraviroc (MVC) and vicriviroc also do not change coreceptor usage from CCR5 to CXCR4, and induce resistance in R5 HIV-1 that harbors several substitutions in the V3 loop and non-V3 regions. In general, the resistant viruses are able to recognize the CCR5 inhibitor-bound form of CCR5 called as non-competitive resistance [14,15,16,17,18,19,20,21] if there are no pre-existing X4 variants [22] though a maraviroc-resistant HIV-1 through competitive resistance mechanisms has been reported *in vivo* [23]. SDF-1α (a natural ligand for CXCR4) and CXCR4 inhibitors such as AMD3100 and T134 also induce selection of inhibitor-resistant variants among X4 viruses without changing coreceptor usage [24,25,26,27,28,29]. Although these resistant variants contain various mutations in multiple regions of gp120, the majority of mutations accumulate in the V3 loop, and some of these mutations are shared in different resistant variants. These observations indicate that the V3 loop is a crucial region for the acquisition of CXCR4-inhibitor resistance. Thus, the V3 loop is also the principal determinant for resistance to natural ligands and coreceptor inhibitors. Conversely, we have previously induced reversion of HIV-1 from dual-X4 to dual-R5 [30] using the CXCR4 inhibitor T140. The reversion is indeed associated with substitution in the 11th position of the V3 loop from arginine to serine [30], which is consistent with the 11/25th rule. Nevertheless, it remains elusive how coreceptor inhibitors induce evolution of HIV-1 to use different coreceptors or acquire resistance. Here, we selected AMD3100-escape variants from a dual-X4 HIV-1

carrying the V3 loop from CRF01_AE, which has no positively charged amino acids at the 11th or 25th positions and lacks an N-linked glycan in the V3 loop, to elucidate HIV-1 evolution for escape from CXCR4 inhibitors.

Materials and Methods

Ethics statement

The study protocol was approved as a part of "the study of immunological and virological analysis in HIV-1 infection (#540) " by the ethics committee for epidemiology and general study in the Faculty of Life Sciences in Kumamoto University and the National Center for Global Health and Medicine. Written informed consent was obtained from all studied individuals according to the Declaration of Helsinki.

Reagents and cells

The CXCR4 antagonist AMD3100 [29,31], CCR5 antagonist MVC [32], and recombinant human sCD4 were supplied by the AIDS Research and Reference Reagent Program, Division of AIDS, National Institute of Allergy and Infectious Diseases (Bethesda, MD, USA). Another CXCR4 inhibitor, T134, was kindly provided by Dr. Hirokazu Tamamura, Tokyo Medical and Dental University, Tokyo, Japan.

The TZM-bl cell line [33] was provided by Dr. John C. Kappes, Dr. Xiaoyun Wu, and Tranzyme through the AIDS Research and Reference Reagent Program, Division of AIDS, National Institute of Allergy and Infectious Diseases, and maintained in Dulbecco's modified Eagle's medium (DMEM) (Sigma) supplemented with 10% fetal bovine serum (FBS) (BioWhittaker). The human embryonic kidney 293T cell line was obtained from American Type Culture Collection (ATCC), and maintained in DMEM supplemented with 10% FBS, 100 U/mL penicillin, and 100 μg/mL streptomycin. The human CD4+ T cell line SupT1 was obtained from ATCC, and its derivative cell line SupT1/CCR5, which expressed high levels of CCR5, was established using a retroviral vector as described previously [13,21], and maintained in RPMI 1640 (Sigma) medium supplemented with 10% FBS, 0.2 mg/mL G418, 100 U/mL penicillin, and 100 μg/mL streptomycin. The CD4-expressing glioma cell line (NP2/CD4) [34,35] was provided by Dr. Hoshino (Gunma University), and its derivative cell lines, NP2/CD4/CXCR4, NP2/CD4/CCR5, and NP2/CD4/CXCR4/CCR5, were established as described previously [13] and maintained in Eagle's minimum essential medium (Sigma) supplemented with 10% FBS and appropriate antibiotics.

Construction of an Env expression vector and infectious molecular clone carrying the V3 loop from CRF01_AE HIV-1

cDNAs of viral RNA from CRF01_AE-infected individuals were prepared as previously described [36]. The *env* region was first amplified using the following primers: 5′-GGTAGAGCAGATGCAGGATG-3′ and 5′-GTGGGTGCTATTCCTAGTGGTTC-3′. Nested PCR was performed using primers carrying *Afl*II and *Nhe*I restriction enzyme sites: 5′-GCACCTTAAGAAATCTGTAGAAATCAATTG-3′ and 5′-GCTAGCTACCTGTTTTAAAGCTTTATACC-3′ (underlines denote *Afl*II and *Nhe*I sites, respectively). The amplified product was then cloned into a pCR-TOPO vector (Invitrogen) and sequenced using an ABI PRISM 3771 automated sequencer (Applied Biosystems). For construction of the Env expression vector carrying the V3 loop from CRF01_AE, the *Afl*II-*Nhe*I fragment of cloned V3 regions was introduced into the *Afl*II-*Nhe*I cloning site of pCXN-JR-FLan [19,20,21]. To construct the infectious molecular clone, the *Afl*II-*Nhe*I fragment was similarly introduced into pJR-FLan [19,20,21] as described previously, resulting in pJR-FLan carrying the V3 loop from CRF01_AE.

Construction of infectious molecular clones and Env expression vectors with mutations

Env expression vectors with single or multiple mutations were constructed using *Dra*III, *Eco*RV, *Nhe*I, and *Bsa*BI sites in KI812.7 *env*. Each PCR fragment carrying a mutation was substituted with wild-type *env*, resulting in an Env expression vector with a single mutation. Env expression vectors with different combinations of mutations were constructed by swapping the restriction fragments. Similarly, infectious molecular clones with mutations were constructed as described previously [19,20,21].

Virus preparation

A pseudotyped virus carrying the luciferase gene was prepared as previously described [13]. Briefly, 293T (3×10^6 cells) were transfected with 20 μg pNL-LucΔBglII and 10 μg pCXN-Env vectors. To produce infectious viral clones, 293T cells were transfected with 30 μg infectious HIV-1 clones. Virus-containing culture supernatants were recovered at 48 h post-transfection, filtered through a 0.22-μm filter (Millipore), and then stored at −80°C until use. The p24 Gag in the supernatant was measured using a p24 Ag ELISA (Zeptometrix) according to the manufacturer's protocol.

Isolation of AMD3100-escape variants from HIV-$1_{JR\text{-}FLan/KI812.7}$

To isolate AMD3100-escape variants from HIV-$1_{JR\text{-}FLan/KI812.7}$, the virus was passaged in SupT1/CCR5 cells with increasing concentrations of AMD3100. Viral replication was monitored by observing the cytopathic effect on SupT1/CCR5 cells. After 21 passages of the virus in SupT1/CCR5 cells at a final AMD3100 concentration of 4 μM, AMD3100 was removed from the virus-infected cell cultures, and the virus was recovered from the culture supernatant. The sensitivity of the escape variant to coreceptor antagonists was determined using TZM-bl cells. DNA was extracted from virus-infected cells using a QIAamp DNA Blood kit (Qiagen) and then subjected to PCR using *Taq* DNA polymerase (Promega). The V3 region sequences were amplified using the following primers: 5′-GCACCTTAAGAAATCTGTAGAAATCAATTG-3′ and 5′-GCTAGCTACCTGTTTTAAAGCTTTATACC-3′. The amplified products were cloned into pCR-TOPO (Invitrogen), and then the *env* regions of the virus were sequenced using the ABI PRISM 3130 automated sequencer.

Determination of drug sensitivity of replication-competent viruses

The sensitivity of replication-competent viruses to coreceptor inhibitors was determined using TZM-bl or SupT1/CCR5 cells. For TZM-bl cells, the cells were infected with viruses at 37°C for 2 days in the presence of various concentrations of coreceptor inhibitors. Luciferase activities of the cells were measured using a luminometer (Lumat LB 9501/16; Berthold). The sensitivity of the virus to coreceptor inhibitors was expressed as the 50% effective concentration (EC_{50}), which was the drug concentration that reduced infection levels by 50% compared with that in the infected, drug-free control of triplicate experiments. For SupT1/CCR5 cells, 5×10^3 cells in U-bottom 96-well microplates were infected with the same amount of virus (100 $TCID_{50}$) in the presence of various AMD3100 concentrations, and then cultured

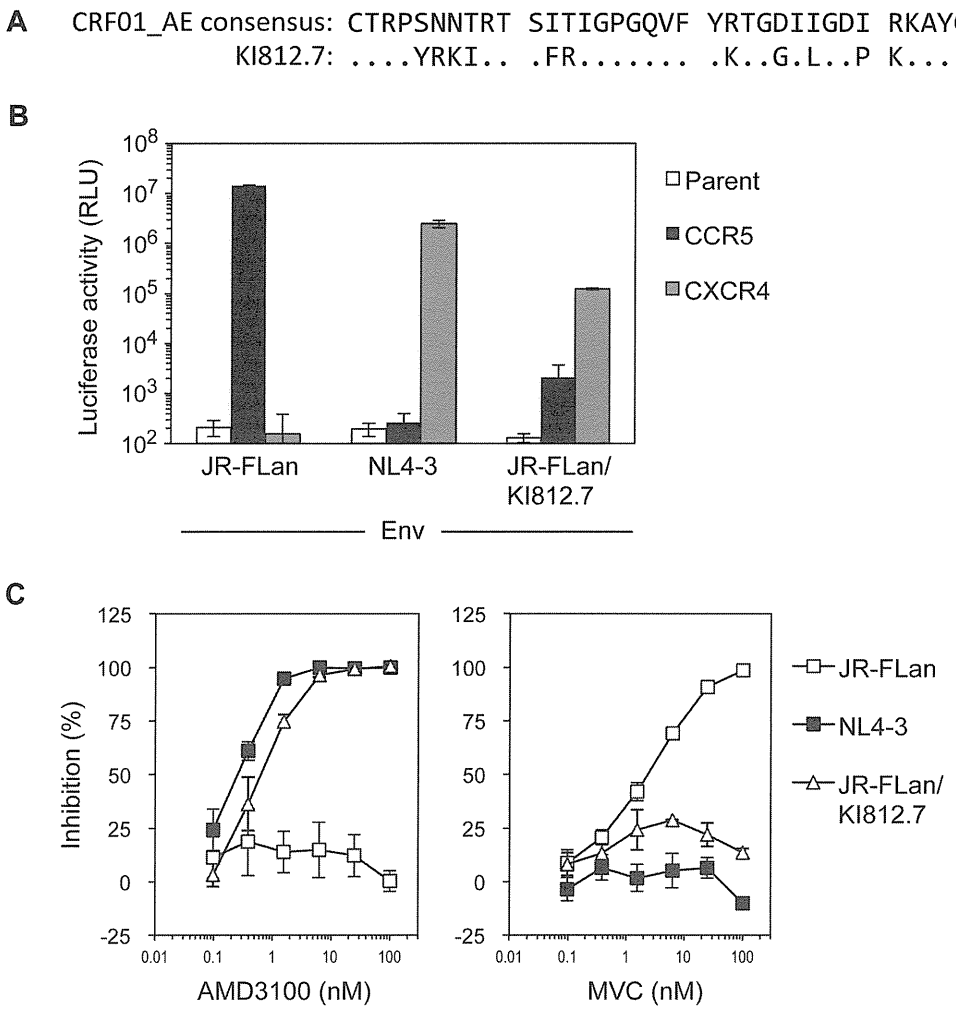

Figure 1. Virological characterization of HIV-1 carrying the V3 loop from CRF01_AE KI812.7. (A) V3 loop amino acid sequences of CRF01_AE consensus and KI812.7. Dots denote sequence identity. (B) Coreceptor usage of JR-FLan carrying the V3 loop from KI812.7. NP2/CD4 cells and NP2/CD4 cells expressing CCR5 or CXCR4 were infected with the same amount of luciferase-reporter pseudotyped virus (10 ng p24Ag). Luciferase activities were measured at 48 h post-infection. Data are the geometric means ± SD of triplicate experiments. (C) Susceptibility of replication-competent HIV-$1_{JR\text{-}FLan/KI812.7}$. TZM-bl cells were infected with replication-competent virus in the presence of AMD3100 or maraviroc (MVC), and then the luciferase activities of the infected cells were measured at 48 h post-infection. Data represent the extent of inhibition of replication relative to that in the absence of AMD3100 or MVC.
doi:10.1371/journal.pone.0089515.g001

for 6 days. The cytopathic effect was determined using an MTT assay as described previously [37].

Determination of drug sensitivity and coreceptor usage of pseudotyped viruses

To determine the coreceptor inhibitor sensitivity of pseudotyped viruses carrying the luciferase gene, NP2/CD4 cells expressing both CCR5 and CXCR4 were used as target cells. Briefly, the target cells (1.5×10^4 cells) were seeded in 48-well culture plates. The following day, the cells were incubated in the presence or absence of various concentrations of coreceptor inhibitors at 37°C for 30 min. The virus (50 ng p24 Ag) was then added to the cells and incubated at 37°C for 48 h. Luciferase activities of the cells were measured using the luminometer. The sensitivity of the virus to coreceptor inhibitors was expressed as the EC_{50}. To examine the coreceptor usage of the virus, NP2/CD4 cells expressing either CCR5 or CXCR4 were infected with pseudotyped viruses carrying the luciferase gene. Luciferase activities were measured after 48 h of infection in triplicate experiments using the luminometer.

Determination of entry efficiency of the virus

Entry efficiency of the virus was determined using a single-round replication assay. Briefly, NP2/CD4/CXCR4/CCR5 cells were infected with the same amount (10 ng p24 Ag) of pseudotyped HIV-1 carrying the luciferase gene. Luciferase activity was measured at 48 h post-infection using the luminometer.

Results

Coreceptor usage of a CRF01_AE-derived HIV-1 and its sensitivity to coreceptor inhibitors

We previously isolated a CXCR4 inhibitor-escape variant from dual-X4 HIV-1 89.6, which has a substitution at the 11th position of the V3 loop [30]. This change does not confer reduced sensitivity to CXCR4 inhibitors, but induces reversion of dual-X4 to dual-R5. However, it remains to be determined how

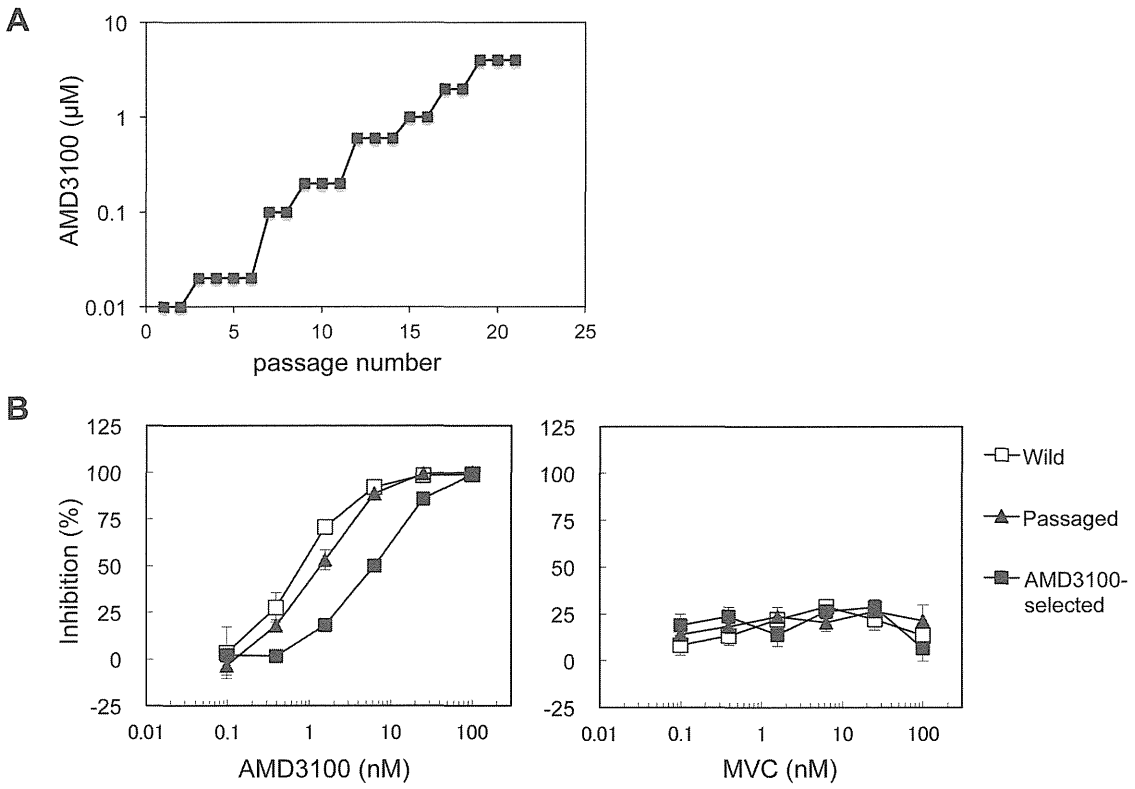

Figure 2. Selection of AMD3100-escape variants from HIV-1$_{JR\text{-}FLan/KI812.7}$. (A) Induction of AMD3100-resistant variants from HIV-1$_{JR\text{-}FLan/KI812.7}$. Replication-competent HIV-1$_{JR\text{-}FLan/KI812.7}$ was passaged using SupT1/CCR5 cells in increasing concentrations of AMD3100 in the range of 20 nM to 4 μM. (B) Susceptibilities of AMD3100-selected variants to AMD3100 and MVC. TZM-bl cells were treated with various concentrations of AMD3100 or MVC, and infected with wild-type HIV-1$_{JR\text{-}FLan/KI812.7}$, the virus passaged in the absence of AMD3100, or the selected virus in the presence of 4 μM AMD3100. Luciferase activities of TZM-bl cells were measured at 48 h post-infection. Data represent the extent of inhibition of replication relative to that in the absence of AMD3100 or MVC.
doi:10.1371/journal.pone.0089515.g002

CXCR4-using HIV-1 without a positively charged amino acid at the 11th position of the V3 loop escapes from CXCR4 inhibitors. Since higher prevalence of CXCR4-using HIV-1 in CRF01_AE compared to subtype B has been reported [38], we first cloned and sequenced the *env* regions of HIV-1s from 21 CRF01_AE-infected individuals in a Japanese cohort to find CXCR4-using HIV-1 lacking positively charged amino acids at the 11th and 25th positions of the V3 loop. Among them, two out of five clones isolated from individual KI812 had a unique amino acid sequence (KI812.7) as shown in Fig. 1A. Although the 11th and 25th positions of the V3 loop did not contain charged amino acids, the net charge of the V3 loop was +7. Furthermore, there was no putative N-linked glycosylation site at the 6th position. Geno2-pheno coreceptor algorithms [39] (http://coreceptor.bioinf.mpi-inf.mpg.de/) predicted that the virus was capable of using CXCR4 as a coreceptor (false positive rate: 0.1%). To confirm the coreceptor usage of the virus, an Env expression vector and an infectious molecular clone carrying the V3 loop derived from KI812.7 were constructed using pJR-FL as a backbone, which were designated as pCXN-FLan/KI812.7 and pJR-FLan/KI812.7, respectively. As we reported previously, the virus pseudotyped with JR-FLan and NL4-3 Env exclusively infected NP2/CD4 cells expressing CCR5 and CXCR4, respectively (Fig. 1B). In contrast, luciferase activity of CXCR4-expressing cells infected with virus carrying FLan/KI812.7 Env was ~100-fold higher than that of CCR5-expressing cells, indicating that FLan/KI812.7 Env preferentially used CXCR4 over CCR5. These results confirmed that substitution of the V3 loop with KI812.7 changed coreceptor usage from R5 to X4 (Fig. 1B). Furthermore, an infectious clone, HIV-1$_{JR\text{-}FLan/KI812.7}$, was sensitive to the CXCR4 inhibitor AMD3100 (EC_{50} value: 0.62±0.21 nM) as well as X4 HIV NL4-3 (EC_{50} value: 0.26±0.04 nM), but resistant to the CCR5 inhibitor MVC in both CCR5- and CXCR4-expressing TZM-bl cells (Fig. 1C). Taken together, the virus carrying JR-FLan/KI812.7 Env was a dual-X4 HIV-1.

Selection of AMD3100-resistant variants from HIV-1$_{JR\text{-}FLan/KI812.7}$

To elucidate how CXCR4-using HIV-1 escapes from the CXCR4 inhibitor AMD3100, we isolated AMD3100-escape variants from HIV-1$_{JR\text{-}FLan/KI812.7}$ using a SupT1 cell line expressing high levels of CCR5. This cell line was able to support both CXCR4- and CCR5-using HIV-1 replication, thereby permitting both resistance to AMD3100 and coreceptor switching of the virus. To select AMD3100-escape variants, SupT1/CCR5 cells were passaged in increasing concentrations of AMD3100. The virus was also passaged in the absence of AMD3100 to exclude the effect of long-term culture. After 21 passages of the virus in the presence of 4 μM AMD3100 (Fig. 2A), the virus was recovered and its sensitivity to AMD3100 was determined using TZM-bl cells. As a result, the selected virus displayed reduced sensitivity (4-fold) to AMD3100 compared with that of the passaged virus in the absence of AMD3100 and the wild-type virus (Fig 2B). The EC_{50} value of the selected virus was 62 nM,

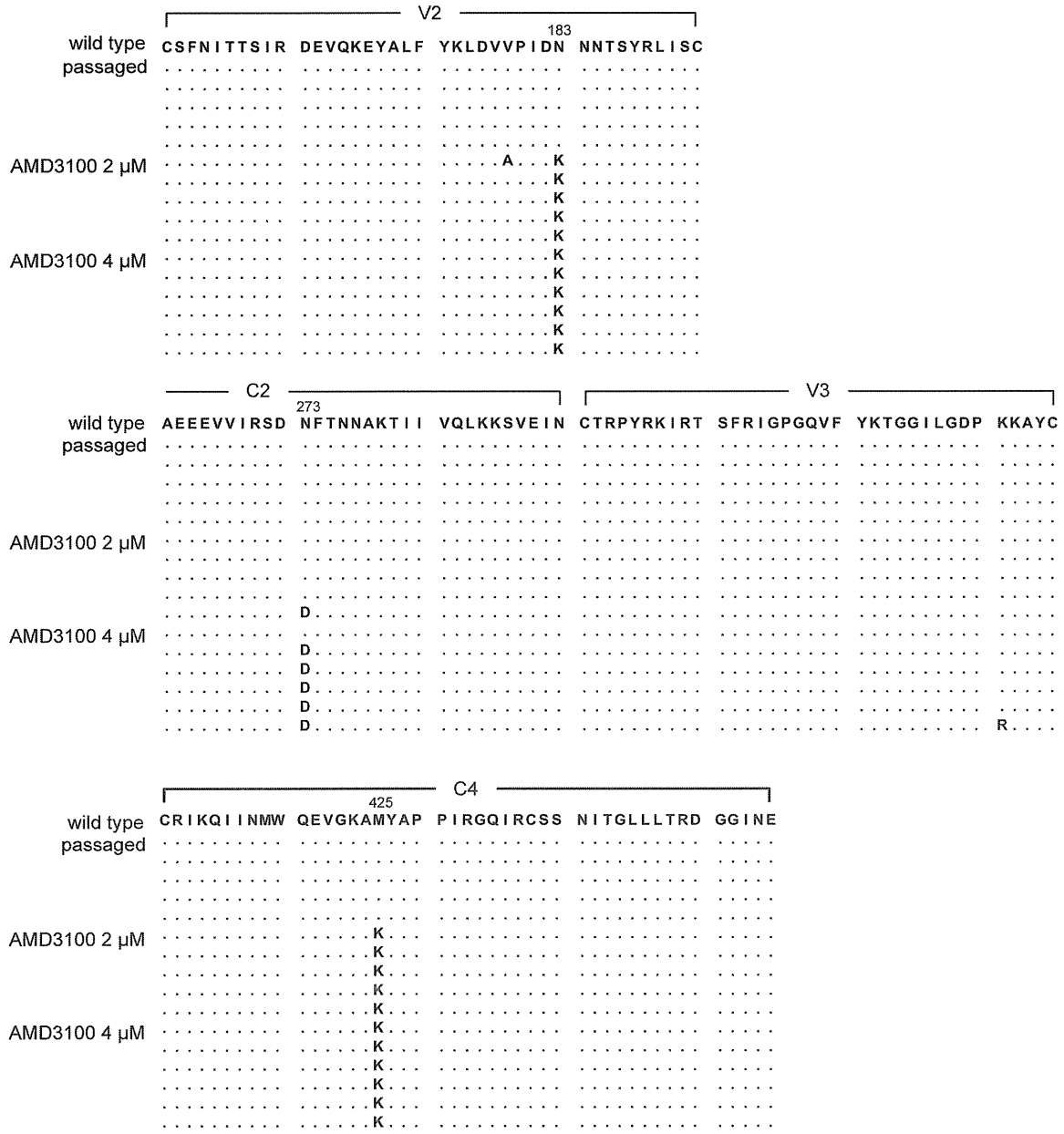

Figure 3. Amino acid sequences of the AMD3100-escape variant. Amplified products from infected SupT1/CCR5 cells in the absence or presence of AMD3100 were cloned, and five to six clones from each sample were sequenced. The amino acid sequences of V2, C2, and C4 of the wild-type HIV-$1_{JR\text{-}FLan/KI812.7}$ are shown in the top line. In each set of clones, the deduced amino acid sequence was aligned by the single amino acid code. Identity with this sequence at individual amino acid positions is indicated by dots.
doi:10.1371/journal.pone.0089515.g003

whereas that of the passaged virus was 14 nM. Furthermore, entry of the selected virus was completely inhibited by high concentrations of AMD3100, and the virus was completely resistant to MVC in TZM-bl cells. These results suggested an absence of coreceptors switching from CXCR4 to CCR5 and a competitive resistance profile of the virus to AMD3100.

Amino acid sequences of the AMD3100-resistant HIV-1

To determine which regions were responsible for the reduced sensitivity of the escape variant to AMD3100, the V1–C4 regions of the envelope gene were sequenced using DNA amplified from infected cells as a template. In the selected virus at 2 μM AMD3100, the virus harbored an N138K substitution in the V2 region and a M425K substitution in the C4 region. Furthermore, the escape variant acquired an N273D substitution in the C2 region at 4 μM AMD3100 (Fig. 3). Most clones passaged in the presence of AMD3100 did not have substitutions in the V3 loop (one clone had a K to R substitution at the 31th position of the V3 loop). In contrast, no remarkable changes were observed in the passaged virus in the absence of AMD3100 (Fig. 3).

Non-V3 regions are involved in the reduced sensitivity to AMD3100

To examine which substitutions were responsible for the reduced sensitivity to AMD3100, we constructed and produced